ISSN 2096-7071
CN 10-1629/R1

CHINA CDC WEEKLY

Vol. 5 No. 26 Jun. 30, 2023

中国疾病预防控制中心周报

COVID-19 ISSUE (39)

ISSN 2096-7071
9 772096 707231 26

China CDC Weekly

Cover Image: poster of International Day Against Drug Abuse and Illicit Trafficking, redesigned by Meng Wang, China CDC Weekly.

Preplanned Studies

Persistent Urinary Tract Infection in Association with Community-Acquired NDM-5 *Escherichia coli* Clonal Group Following COVID-19 Infection — Beijing Municipality, China, 2023

Jiazhen Guo[1,&]; Ran Duan[2,&]; Dan Zhang[2]; Peng Zhang[2]; Shuai Qin[2]; Yajuan Fang[1]; Yingna Sun[1]; Lianhe Lu[1]; Huaiqi Jing[2]; Xin Wang[2,#]; Rongmeng Jiang[1,#]; Biao Kan[3,#]

Summary

What is already known about this topic?

The hospital-acquired infections caused by New Delhi metallo-beta-lactamase (NDM)-producing strains are typically attributed to a single clonal lineage.

What is added by this report?

In this study, we encountered a unique case of community-acquired NDM-5 *Escherichia coli* urinary tract infection (UTI) following coronavirus disease 2019 (COVID-19). The UTI persisted for a duration of at least 45 days. Genomic analyses revealed the presence of two NDM-5 strains, both sharing an identical chromosomal background but distinct, homologous, and recombined plasmids. This case suggests that a diverse range of resistance genes may be present within the human body, with drug-resistant strains undergoing continuous evolution during infection. The intestinal tract may have been its drug-resistant gene pool.

What are the implications for public health practice?

The observations presented in this case indicate that the endogenous acquisition of drug-resistant genes may also be an issue in managing multidrug-resistant organisms (MDRO). It is possible for continuous recombination to occur within carbapenem-resistant Enterobacteriaceae (CRE) during infection. In contrast to exogenously-acquired resistance, greater attention should be placed on the endogenous factors that contribute to the development of CRE within healthcare settings.

Carbapenem-resistant Enterobacteriaceae (CRE) infections, specifically those involving New Delhi metallo-beta-lactamase (NDM) drug-resistant bacteria, continue to pose challenges for healthcare institutions. High-risk coronavirus disease 2019 (COVID-19) patients are susceptible to developing secondary bacterial coinfections, with CRE coinfections reportedly having significant implications for COVID-19 prognosis. In this report, we present a unique case of a NDM-producing bacterial coinfection following COVID-19 infection.

In late December 2022, a hospital in Beijing admitted an elderly female patient who had been infected with COVID-19 for three weeks. Subsequent laboratory tests revealed a persistent urinary tract infection (UTI) lasting over 45 days, caused by community-acquired NDM-5 *Escherichia coli*. Genomic analyses demonstrated that the infection was not the result of a single strain but rather a group of clonally related, chromosomally indistinguishable *E. coli* strains with varying acquisitions or losses of drug-resistance plasmids. During the course of the infection, a novel drug-resistance plasmid recombined within the patient.

This case highlights the continuous evolution of drug-resistant bacterial strains during infections and suggests that the intestinal tract may serve as a source for the gene pool.

A unique case was identified in a hospital in Beijing involving a patient admitted from December 29, 2022, to January 13, 2023. CRE *E. coli* was isolated from both the patient's sputum and urine on December 31, 2022. Medical records and clinical test results were collected for analysis. The patient was followed up twice to isolate the multidrug-resistant organisms (MDRO): urine and feces samples were collected on January 26, 2023, and additional urine, feces, and sputum samples were obtained on February 17, 2023. A urine routine test was also conducted on February 17, 2023. Concurrently, control samples were collected from the patient's live-in nanny on February 17, 2023.

The antibiotic sensitivity of the strains was evaluated using minimum inhibitory concentrations (MICs) testing using VITEK® 2 COMPACT (bioMérieux, Marcy-l'Étoile, France), and bla_{NDM} genes were detected and sequenced in positive samples (*1*). All strains underwent molecular typing with MLST (*2*), and whole-genome sequencing was carried out using

PacBio Sequel (Pacific Biosciences, Menlo Park, USA) and Illumina NovaSeq (Illumina, San Diego, USA) technologies. Antibiotic resistance genes were predicted using ResFinder 4.1 (Technical University of Denmark, Kongens Lyngby, Denmark) (*3*).

Genomic synteny between two plasmids was visualized using ACT release 13.0.0 (Wellcome Trust Sanger Institute, Cambridge, UK). Primers were designed and amplified for all assembled plasmids identified through whole-genome analysis (Supplementary Table S1, available in https://weekly.chinacdc.cn/). A phylogenetic tree based on the core chromosomal genome was constructed using the neighbor-joining method (*4*–*6*). Additionally, a NJ tree for plasmids and associated megaBLAST hits was developed based on pairwise alignments.

The patient, a 93-year-old woman with a smoking history of over 75 years, tested positive for COVID-19 antigen three weeks prior. In early and mid-December 2022, she experienced a fever that peaked at 38.7 ℃, accompanied by mild chills. At that time, she was severe acute respiratory syndrome coronavirus 2 (SARS-CoV-2) antigen-positive. Subsequently, her body temperature returned to normal without the use of antipyretics. She self-medicated with a second-generation cephalosporin antibiotic for three weeks without medical consultation. Around December 20, 2022, she sustained burns to her neck, face, and auricle due to smoking while inhaling oxygen at home. Approximately two days later, she developed a low-grade fever, exhibited a decreased appetite, and showed signs of mental fatigue.

On December 29, 2022, the patient was admitted to the hospital for persistent discomfort following the COVID-19 infection and neck and facial burns. She did not report any urinary tract discomfort during admission or hospitalization and denied any abnormal discharge. On the day of admission, PCR tests for SARS-CoV-2, influenza A, influenza A (H1N1), seasonal influenza A (H3), and influenza B were all negative, and antibody testing for *Mycoplasma pneumoniae* was also negative. As the SARS-CoV-2 infection had resolved at least two weeks prior, Paxlovid was not indicated. The treatment focused on maintaining oxygenation status, managing water and electrolyte balance, and addressing the skin burns.

Due to elevated blood neutrophil levels on admission (Table 1), a bacterial infection was suspected. Consequently, moxifloxacin was added to the treatment regimen at a dosage of 0.4 g

TABLE 1. Significant clinical test results for the patient following COVID-19 infection — Beijing, China, 2023.

Clinical tests	December 29, 2022	December 31, 2022	January 5, 2023	January 9, 2023	February 17, 2023
Blood					
White blood cell	8.95×10^9	9.85×10^9	5.6×10^9	5.81×10^9	–
Neutrophil count	7.03×10^9	8.49×10^9	3.71×10^9	3.85×10^9	–
Neutrophil (%)	78.50	86.20	66.10	66.20	–
Lymphocyte count	1.03×10^9	0.79×10^9	1.2×10^9	1.15×10^9	–
Lymphocyte (%)	11.50	8.00	21.40	19.80	–
Monocytes count	0.82×10^9	0.53×10^9	0.58×10^9	0.62×10^9	–
Monocytes (%)	9.20	5.44	10.30	10.70	–
ESR (mm/h)	65	–	74	–	–
CK (U/L)	102.6	280.8	74.3	–	–
CRP (mg/L)	56.3	94.0	8.8	6.4	–
SAA (mg/L)	311.8	392.2	66.9	23.6	–
PCT (ng/L)	<0.05	<0.05	<0.05	<0.05	–
D-Dimer (mg/L)	3.10	–	1.21	1.07	–
Urine					
Leukocytes in the urine (p/HPF)	–	128.77	104.03	14.48	168.83
Red blood cells in the urine (p/HPF)	–	1.40	3.56	5.19	0.96
Bacteria count in the urine (p/HPF)	–	3177.32	912.81	729.26	1002.55

Note: "–" means data not available.
Abbreviation: ESR=erythrocyte sedimentation rate; CK=creatine kinase; CRP=C reactive protein; SAA=serum amyloid A; PCT=procalcitonin.

intravenously per day, commencing on December 31, 2022, and ceasing on January 6, 2023. The patient was discharged on January 13, 2023, due to improvement in her condition.

CRE was isolated from the patient's urine and sputum on December 31, 2022, from her urine on January 5, 2023, and from her urine and feces on January 26, 2023, and February 17, 2023. No CRE was isolated from the patient's live-in nanny at any time point. All strains isolated from the patient carried the *bla*$_{NDM}$-5 gene (accession numbers OQ357728, OQ357729, OQ442328, OQ442329, OQ442330, OQ851640, and OQ851641). The antimicrobial resistance spectra of NDM-5-producing *E. coli* indicated two types, which differed between the strains isolated from urine and sputum on December 31, 2022, with respect to gentamicin, tobramycin, and trimethoprim/sulfamethoxazole (Table 2). To exclude non-CRE *E. coli* infection, the *bla*$_{NDM}$ gene positivity rate among 95 *E. coli* isolates acquired from urine on February 17, 2023, was determined to be 88.42%. The antimicrobial resistance results for gentamicin, tobramycin, and trimethoprim/sulfamethoxazole of these NDM-producing *E. coli* isolates were identical (Table 2). The patient was admitted to a new ward that opened on December 21, 2022. No MDRO had been detected in the ward's environment or among other patients from the ward's opening until four weeks after the patient with NDM-5-producing *E. coli* was discharged (December 21, 2022 to February 10, 2023). The patient had not been hospitalized in the past three years, suggesting that the NDM-5-producing *E. coli* was community-acquired.

A group of NDM-5-producing *E. coli* strains were isolated four times from a patient, and they shared the same chromosomes (CP123592, CP123593). Each of these strains carried four plasmids, three of which were identical: pDJH_Plas_NDM-5 (CP123590), pDJH_Plas3 (CP123589), and pDJH_Plas4 (CP123594). The distinct plasmids were pDJH_137urine_Plas1 (CP123591) and pDJH_183sputum_Plas2 (CP123595) (Supplementary Table S2, available in https://weekly.chinacdc.cn/). Figure 1 displays the timeline of strain isolation, genomic composition, and homology analysis.

All NDM-5 *E. coli* strain sequence types were identified as ST 410, which is distinct from the common uropathogenic *E. coli* (UPEC) strains. The chromosome size was 4.8 Mb, with a G+C content of 50.67 mol%. A NJ tree, including the five sequenced strains and representative strains from each lineage, was divided into two branches. The *E. coli* chromosome in this study was part of branch C, which was relatively distant from most UPEC strains. The nearest human strain was enteroinvasive *E. coli* (EIEC) with a chromosome size of 4.8 Mb and G+C content of 50.7 mol%.

Common virulence factors of UPEC such as *fimH*, *afa*, *fyuA*, *hlyA*, *iucABCD*, *kpsF*, and *sfa* were found within the chromosome. Notably, type I fimbriae (*fimH*) plays a crucial role in UPEC's ability to colonize the urethral epithelium and migrate to the bladder. Additionally, the chromosome encodes for the locus of enterocyte effacement (LEE) (*7*–*8*).

The pDJH_Plas_NDM-5 is a 48Kbp IncX3 plasmid that carries the *bla*$_{NDM-5}$ gene. It has a similar backbone to *bla*$_{NDM-5}$ plasmids of various sources, which range from 46,155 to 53,056 bp in size, with 84% (42/50) of them being 46,161 bp. None of the top 50 megaBlast hits was the same size as Plas_NDM-5 of 48,020 bp. The extra sequences in this case encoded IS91 family transposase and a putative protein of unknown function. pDJH_Plas_NDM-5 plasmid remained stable after 70 passages in vitro.

The pDJH_183sputum_Plas2 plasmid (48.6 Kbp) exhibited 31.87% coverage and 99.78% identity when compared with pDJH_137urine_Plas1 (152.2 Kbp), suggesting their homology. The top megaBLAST hit demonstrated 96% coverage and 99.87% identity with pDJH_183sputum_Plas2. In contrast, the top hit for pDJH_137urine_Plas1 revealed only 67% coverage, implying that it was not a pre-existing plasmid but rather a newly emerged plasmid. The pDJH_183sputum_Plas2 plasmid encodes the blaTEM-1B gene, which mediates resistance to ampicillin, cephalothin, piperacillin, and ticarcillin. The pDJH_137urine_Plas1 plasmid encodes 11 resistance genes that mediate resistance to 30 types of antibiotics across seven categories: sulfonamides, aminoglycosides, phosphomycin, macrolides, tetracyclines, β-lactams, and acyl alcohol.

The differences in drug resistance between strains DJH_183sputum and DJH_137urine (Table 2), specifically concerning compound sulfonamides, gentamicin, and tobramycin, were attributed to the presence of *dfrA12*, *sul2*, and *aac(3)-IV*, which were exclusively found in the pDJH_137urine_Plas1 plasmid. Therefore, it was deduced that pDJH_137urine_Plas1 originated from recombination with pDJH_183sputum_Plas2 and acquired new resistance genes within the patient's body. Initially, on December 31, 2022, the patient's urine and sputum strains carried these two plasmids, respectively. On January 5, 2023, the urine strain (JARVKQ0000 00000) harbored pDJH_137urine_Plas1. However,

TABLE 2. Spectrum of antibiotic resistance among *bla*$_{NDM-5}$ strains isolated from the patient following COVID-19 infection — Beijing, China, 2023.

Antibiotic	December 31, 2022				January 5, 2023		January 26, 2023				February 17, 2023			
	Urine		Sputum		Urine		Urine		Feces		Urine		Feces	
	MIC (μg/mL)	Interpretation	MIC (μg/mL)	Interpretation	MIC (μg/mL)	Interpretation	MIC (μg/mL)	Interpretation	MIC (μg/mL)	Interpretation	MIC (μg/mL)	Interpretation	MIC (μg/mL)	Interpretation
Ampicillin	≥32	R	≥32	R	≥32	R	≥32	R	≥32	R	≥32	R	≥32	R
Ampicillin/sulbactam	≥32	R	≥32	R	≥32	R	≥32	R	≥32	R	≥32	R	≥32	R
Piperacillin/tazobactam	≥128	R	≥128	R	≥128	R	≥128	R	≥128	R	≥128	R	≥128	R
Cefazolin	≥64	R	≥64	R	≥64	R	≥64	R	≥64	R	≥64	R	≥64	R
Cefotetan	≥64	R	≥64	R	≥64	R	≥64	R	≥64	R	≥64	R	≥64	R
Ceftazidime	≥64	R	≥64	R	≥64	R	≥64	R	≥64	R	≥64	R	≥64	R
Ceftriaxone	≥64	R	≥64	R	≥64	R	≥64	R	≥64	R	≥64	R	≥64	R
Cefepime	≥64	R	≥64	R	≥64	R	≥64	R	≥64	R	≥64	R	≥64	R
Aztreonam	≥64	R	16	R	≥64	R	16	R	16	R	16	R	16	R
Ertapenem	≥8	R	≥8	R	≥8	R	≥8	R	≥8	R	≥8	R	≥8	R
Imipenem	≥16	R	≥16	R	≥16	R	≥16	R	≥16	R	≥16	R	≥16	R
Amikacin	≤2	S	≤2	S	≤2	S	≤2	S	≤2	S	≤2	S	≤2	S
Gentamicin	≥16	R	≤1	S	≥16	R	≤1	S	≤1	S	≤1	S	≤1	S
Tobramycin	≥16	R	≤1	S	≥16	R	≤1	S	≤1	S	≤1	S	≤1	S
Ciprofloxacin	≥4	R	≥4	R	≥4	R	≥4	R	≥4	R	≥4	R	≥4	R
Levofloxacin	≥8	R	≥8	R	≥8	R	≥8	R	≥8	R	≥8	R	≥8	R
Nitrofurantoin	≤16	S	≤16	S	≤16	S	≤16	S	≤16	S	≤16	S	≤16	S
Trimethoprim/ Sulfamethoxazole	≥320	R	≤20	S	≥320	R	≤20	S	≤20	S	≤20	S	≤20	S

Note: S=sensitive; R=resistant; MIC=minimum inhibitory concentration.

after January 26, 2023, only pDJH_183sputum_Plas2 was detected in isolated strains (JARVKR000000000, JARVKS000000000), indicating that pDJH_137urine_Plas1 was not stably maintained, while pDJH_183sputum_Plas2 was (Figure 1A).

The other two plasmids, pDJH_Plas3 (96.2 Kbp) and pDJH_Plas4 (4.4 Kbp), do not carry any resistance genes.

A.

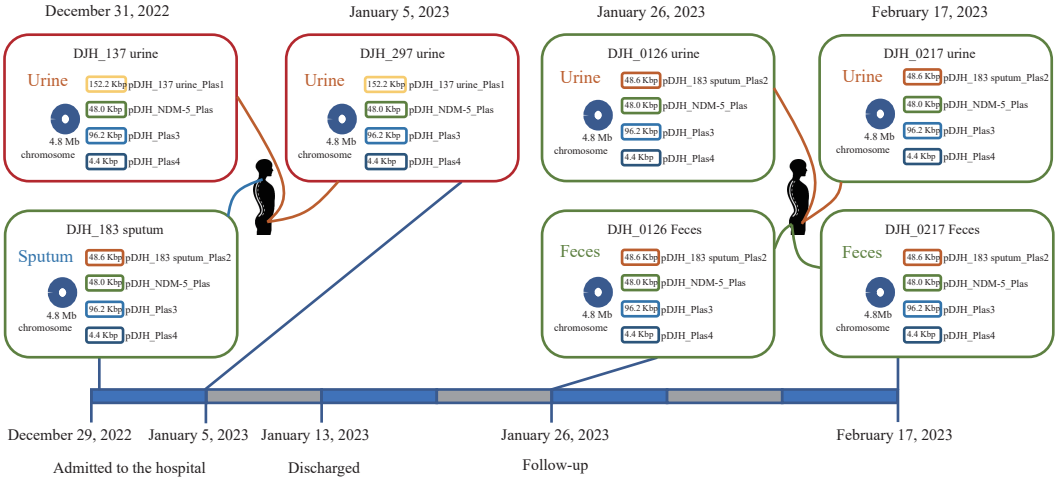

B.

Characteristic	Chromo-some	Plasmids of DJH_183_sputum				
		Plasmids of DJH_137 urine				
		pDJH_137 urine_Plas1	pDJH_Plas_NDM-5	pDJH_Plas 3	pDJH_Plas 4	pDJH_183 sputum_Plas2
Genome size	4.8 Mb	152.2 Kbp	48.0 Kbp	96.2 Kbp	4.4 Kbp	48.6 Kbp
GC%	50.7	51.5	47	50.2	55.5	50.6
Aver CDS	909.9	716.8	640.9	680.3	426	685.3
CDS%	87.3	80.1	86.8	79.9	29.3	81.7
IS(Family)	89(20)	102(20)	32(20)	4(1)	0	34(20)

C.

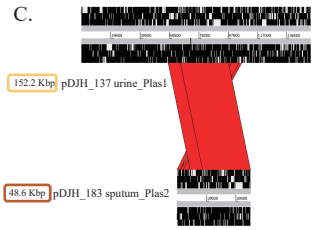

D.

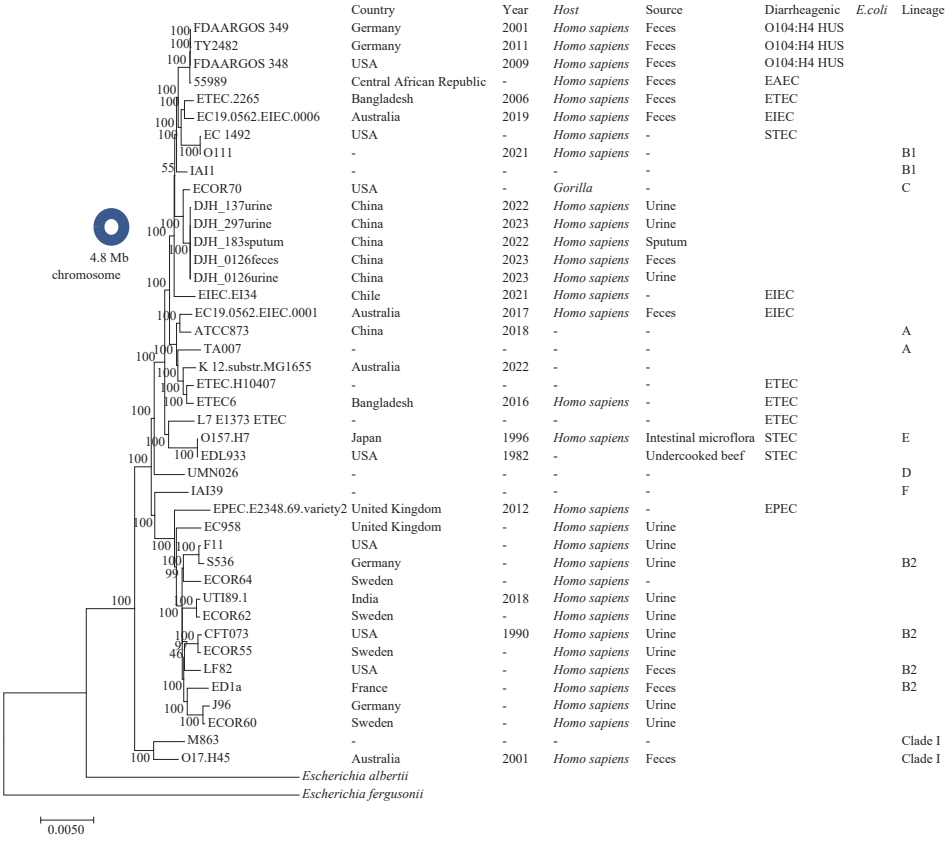

FIGURE 1. Comparative genome analysis and timeline of the isolation of *bla*$_{NDM-5}$ *E. coli* strains from the patient following COVID-19 infection — Beijing, China, 2023. (A) Isolation source and genomic composition of the strains. (B) Genomic properties of the chromosome and plasmids of the strains isolated on December 31, 2022. (C) Genomic synteny between pDJH_137urine_Plas1 and pDJH_183sputum_Plas2 plasmids. (D) Neighbor-joining tree based on the core genome of the *E. coli* strains isolated on December 31, 2022, January 5, 2023, and January 26, 2023, and *E. coli* representatives from each phylogroup. (E) Neighbor-joining tree of pDJH_137urine_Plas1 and the top 50 megaBLAST hits using BLAST pairwise alignments. (F) Neighbor-joining tree of pDJH_183sputum_Plas2 and the top 50 megaBLAST hits using BLAST pairwise alignments. (G) Neighbor-joining tree of pDJH_Plas_NDM-5 and the top 50 megaBLAST hits using BLAST pairwise alignments. (H) Neighbor-joining tree of pDJH_Plas3 and the top 50 megaBLAST hits using BLAST pairwise alignments. (I) Neighbor-joining tree of pDJH_Plas4 and the top 50 megaBLAST hits using BLAST pairwise alignments.
Abbreviation: IS=Insertion Sequence; EAEC=Enteroaggregative *Escherichia coli*; ETEC=Enterotoxigenic *Escherichia coli*; EIEC=Enteroinvasive *Escherichia coli*; STEC=Shiga toxin-producing *Escherichia coli*.

DISCUSSION

The diagnostic criteria for a UTI include clinical symptoms and the presence of a pathogen. Pyuria, or the presence of white blood cells or pus in the urine, serves as a significant indicator (*9*). Although the patient in this study did not report any subjective UTI symptoms, NDM-5 *E. coli* was isolated from her urine four times over a period of 45 days, accompanied by noticeable bacteriuria and pyuria (Table 1). Consequently, a diagnosis of persistent UTI was made. The NDM-5 *E. coli* infection in this case was likely community-acquired, with the bacteria being selectively eliminated in vivo due to the patient's at-

home use of a second-generation cephalosporin. The spread of the bacterial strains appeared to be limited, as the patient's nanny did not contract the infection.

Interestingly, the NDM-5 *E. coli* was not a single clone but rather a group of homologous *E. coli* strains. These strains possessed the same chromosome but carried different plasmids and were present concurrently in multiple systems (e.g., the urethra and the respiratory tract, the urethra and the intestinal tract). Following the cessation of antibiotics, the pDJH_137urine_Plas1 plasmid, which conferred a broader drug resistance spectrum, gradually disappeared. In contrast, the less-drug-resistant plasmid pDJH_183sputum_plasmid2 remained within the NDM-5 *E. coli* population (Figure 1A).

The source of the patient's infection was investigated by collecting and analyzing their fecal samples twice after their discharge from the facility. In both instances, NDM-5 *E. coli* strains were isolated. Previous research has identified the intestinal tract as a reservoir for antibiotic-resistance genes (*1*,*10*). The patient also reported habitually wiping her perineal area from back to front after bowel movements. It was hypothesized that the *E. coli* strains' plasmids underwent recombination within the gastrointestinal tract and were subsequently transferred to the urinary tract due to the patient's wiping habit. Virulence genes, such as *fimH*, facilitated the strains' colonization along the epithelial cells of the urinary tract. Coincidentally, the bacterial strain carrying the NDM-5 plasmid, which conferred extensive antibiotic resistance, led to a persistent UTI.

In the present case, a rare occurrence of community-acquired NDM-5 *E. coli* UTI persisted for over 45 days. Two NDM-5 strains were identified, both having the same chromosome but with homologous and recombined plasmids. This finding suggests that multidrug-resistant bacteria were not stable throughout the infection. While new plasmids can be acquired, the plasmids themselves may also undergo constant recombination, leading to variations in antibiotic resistance profiles. This case implies that a diverse range of resistance genes may be intrinsic to the human body, and the CRE could undergo recombination as a consequence of environmental pressures, such as those imposed by antibiotic usage. The intestinal tract might serve as the source of the gene pool. Therefore, in contrast to exogenous infection, more attention should be given to endogenous factors contributing to the development of CRE.

Conflicts of interest: No conflicts of interest.

Acknowledgements: Charlesworth Author Services (Paper no.117766) for their critical editing and helpful comments regarding our manuscript.

Funding: Supported by the National Key Research and Development Program of China (2022YFC2602203).

doi: 10.46234/ccdcw2023.110

[#] Corresponding authors: Xin Wang, wangxin@icdc.cn; Rongmeng Jiang, rongmengj@163.com; Biao Kan, kanbiao@icdc.cn.

[1] Beijing Ditan Hospital Capital Medical University, Beijing, China; [2] National Institute for Communicable Disease Control and Prevention, Chinese Center for Disease Control and Prevention, Beijing, China; [3] State Key Laboratory of Infectious Disease Prevention and Control, Beijing, China.
[&] Joint first authors.

Submitted: May 14, 2023; Accepted: June 20, 2023

REFERENCES

1. Lv DY, Duan R, Fan R, Mu H, Liang JR, Xiao M, et al. *bla*$_{NDM}$ and *mcr-1* to *mcr-5* gene distribution characteristics in gut specimens from different regions of China. Antibiotics (Basel) 2021;10(3):233. http://dx.doi.org/10.3390/antibiotics10030233.
2. Zhou ZM, Alikhan NF, Mohamed K, Fan YL, Agama Study Group, Achtman M. The EnteroBase user's guide, with case studies on *Salmonella* transmissions, *Yersinia pestis* phylogeny, and *Escherichia* core genomic diversity. Genome Res 2020;30(1):138 – 52. http://dx.doi.org/10.1101/gr.251678.119.
3. Bortolaia V, Kaas RS, Ruppe E, Roberts MC, Schwarz S, Cattoir V, et al. ResFinder 4. 0 for predictions of phenotypes from genotypes. J Antimicrob Chemother 2020;75(12):3491 – 500. http://dx.doi.org/10.1093/jac/dkaa345.
4. Clermont O, Christenson JK, Denamur E, Gordon DM. The Clermont *Escherichia coli* phylo-typing method revisited: improvement of specificity and detection of new phylo-groups. Environ Microbiol Rep 2013;5(1):58 – 65. http://dx.doi.org/10.1111/1758-2229.12019.
5. Le Gall T, Clermont O, Gouriou S, Picard B, Nassif X, Denamur E, et al. Extraintestinal virulence is a coincidental by-product of commensalism in B2 phylogenetic group *Escherichia coli* strains. Mol Biol Evol 2007;24(11):2373 – 84. http://dx.doi.org/10.1093/molbev/msm172.
6. Brons JK, Vink SN, de Vos MGJ, Reuter S, Dobrindt U, van Elsas JD. Fast identification of *Escherichia coli* in urinary tract infections using a virulence gene based PCR approach in a novel thermal cycler. J Microbiol Methods 2020;169:105799. http://dx.doi.org/10.1016/j.mimet.2019.105799.
7. Lin WH, Wang MC, Liu PY, Chen PS, Wen LL, Teng CH, et al. *Escherichia coli* urinary tract infections: host age-related differences in bacterial virulence factors and antimicrobial susceptibility. J Microbiol Immunol Infect 2022;55(2):249 – 56. http://dx.doi.org/10.1016/j.jmii.2021.04.001.
8. Bunduki GK, Heinz E, Phiri VS, Noah P, Feasey N, Musaya J. Virulence factors and antimicrobial resistance of uropathogenic *Escherichia coli* (UPEC) isolated from urinary tract infections: a systematic review and meta-analysis. BMC Infect Dis 2021;21(1):753. http://dx.doi.org/10.1186/s12879-021-06435-7.
9. Semeniuk H, Church D. Evaluation of the leukocyte esterase and nitrite urine dipstick screening tests for detection of bacteriuria in women with suspected uncomplicated urinary tract infections. J Clin Microbiol 1999;37(9):3051 – 2. http://dx.doi.org/10.1128/jcm.37.9.3051-3052.1999.
10. Kent AG, Vill AC, Shi QJ, Satlin MJ, Brito IL. Widespread transfer of mobile antibiotic resistance genes within individual gut microbiomes revealed through bacterial Hi-C. Nat Commun 2020;11(1):4379. http://dx.doi.org/10.1038/s41467-020-18164-7.

SUPPLEMENTARY MATERIALS

SUPPLEMENTARY TABLE S1. Specific primers for individual plasmids and shared primers for pDJH_137urine_Plas1 and pDJH_183sputum_Plas2.

Target plasmid	Primer name	5'→3' sequence	Amplicon length (bp)
pDJH_137urine_Plas1	S137P1-F1	TTTTGCCGTTACGCACCACTC	1,033
	S137P1-R1	CGCCCTGCCTCTTACTCTACT	
	S137P1-F2	AAAACGGCAAACCAGTCCTCA	504
	S137P1-R2	CAAACGGTCTTACTCCATTCA	
pDJH_183sputum_Plas2	183_plas2F	ATGGCAAACTGAAACGG	616
	183_plas2R	CCTGTCCCTACACCAATAA	
	183P2-5F	GGCTTACGCCACCATCAAAG	287
	183P2-5R	TACGCCAAGACGAACCATCA	
pDJH_Plas_NDM-5	S137P2-ndm-F1	GCGTAGCGTTTCCATAGCG	678
	S137P2-ndm-R1	CGAGGTCTTCGTCCTGTCC	
	S137P2-ndm-F2	CCACGACAGCCAGGAGT	522
	S137P2-ndm-R2	TTCGGGCGGTTTAGTTT	
pDJH_Plas3	S183P3-F1	AAGGCGCTTTCTGATTTGG	667
	S183P3-R1	CGCTACCTGGGTCGTTATCT	
	S183P3-F2	CCACGCTGATGGAACTGAA	941
	S183P3-R2	GCGGAGGTCTGAATAAACACG	
pDJH_Plas4	S137P4-F1	CACATTCGCTCGCTACGCT	816
	S137P4-R1	CACGCTCACCTGCTATACGC	
	S137P4-F2	CAGTCGCTTACACTACACCCA	1,175
	S137P4-R2	GGCAGGATAACCCGCTACAT	
pDJH_137urine_Plas1 pDJH_183sputum_Plas2	S183P2-F1	AGATAACGACCCAGGTAGCG	799
	S183P2-R1	AACTGAAGCGGAGATGAAGG	
	S183P2-F2	TACCGCTGTCCACGCCTTAT	598
	S183P2-R2	CACGCTACCTGGGTCGTTATCT	

SUPPLEMENTARY TABLE S2. Presence of the plasmids in *bla*$_{NDM-5}$ *E. coli* from a UTI patient.

Plasmid	December 31, 2022		January 5, 2023	January 26, 2023		February 17, 2023	
	Urine	Sputum	Urine	Urine	Feces	Urine	Feces
pDJH_137urine_Plas1	+	−	+	−		−	
pDJH_183sputum_Plas2	−	+	−	+		+	
pDJH_Plas_NDM-5	+	+	+	+		+	
pDJH_Plas3	+	+	+	+		+	
pDJH_Plas4	+	+	+	+		+	

Note: "+" means positive; "−" means negative.

Preplanned Studies

Medical Consultations Option and Influencing Factors for SARS-CoV-2 Infected Individuals — Beijing Municipality, China, December 2022

Mingyue Li[1]; Jue Liu[2]; Ming Du[2]; Chen Wang[3]; Yafang Huang[1]; Wentao Li[1]; Tong Xiang[1]; Jingwei Zhao[1]; Xiaoli Zhu[4]; Xinying Dong[4]; Hao Wu[1,#]; Shugang Li[4,#]

Summary

What is already known about this topic?

In December 2022, China revised its epidemic prevention and control strategy, leading to an increase in coronavirus disease 2019 (COVID-19) cases and a peak in medical consultations. Government departments implemented relevant policies to coordinate and allocate medical resources throughout China. However, there is a scarcity of research on the status of medical consultations and the factors influencing them.

What is added by this report?

In the study population, over 80% of individuals with COVID-19 chose not to pursue medical care, while more than 70% of patients who sought treatment opted for primary healthcare facilities. The decision to consult medical professionals was influenced by various factors, such as age, education level, employment status, urban-rural distribution, and the presence of symptoms following COVID-19 infection.

What are the implications for public health practice?

The implementation of tiered diagnostic and treatment approaches, aligned with guidelines issued by governing bodies, is essential for mitigating the strain on medical resources. Primary healthcare institutions serve as "gatekeepers" for public health and should be further expanded in the future.

In December 2022, the Joint Prevention and Control Mechanism of the State Council issued the *Notice on Further Optimizing the Implementation* of *COVID-19 Prevention and Control Measures*. The notice emphasized that the virulence of the Omicron strain had decreased, with clinical observations indicating that most infections resulted in asymptomatic or mild symptoms (*1*). Concurrently, the government devised targeted prevention, control, and treatment strategies for specific populations (*2*). Following the adjustment of these policies, the number of infected individuals experienced fluctuations, reaching a peak shortly after the new measures were implemented. As of December 23, 2022, fever clinics across the nation recorded a cumulative total of 2.867 million consultations and treatments (*3*). Consequently, the effective allocation of medical resources and the provision of high-quality, tiered diagnosis and treatment for coronavirus disease 2019 (COVID-19) patients have emerged as significant public health concerns warranting attention from relevant departments.

Supported by the Beijing Municipal Health Commission, a cross-sectional questionnaire survey was conducted at 354 community health service centers across 16 districts in Beijing. A random sampling method was employed, which was based on the population proportion within each district. From December 26 to December 31, 2022, a total of 33,968 infected individuals participated in the study. Eligible participants met the following inclusion criteria: 1) confirmed COVID-19 diagnosis through nucleic acid or antigen tests, or reported symptoms of COVID-19; 2) aged 18 years or older; and 3) willingness to participate in the survey and provide informed consent. Those who refused participation were not included in the study.

The study obtained data on fundamental demographic characteristics, post-infection symptoms, comorbidities, treatment modalities, and healthcare pathway selection. To delineate the treatment landscape, the 33,968 patients were classified into 2 cohorts: those who underwent treatment and those who did not. Treatment types were further segregated into 3 categories: primary care facilities, hospitals, and a combination of both. R software (version 4.2.2, R Foundation for Statistical Computing, Vienna, Austria) was employed for data analysis and

visualization. Count data are expressed as composition ratios or percentages. Statistical analyses were conducted to investigate the factors influencing consultation rates and treatment preferences. Moreover, variables exhibiting statistical significance in univariate analysis were incorporated into a multivariate logistic regression model to compute odds ratios (*OR*) and 95% confidence intervals (*CI*). $P<0.05$ was considered the threshold for statistical significance.

In this study, it was found that out of 33,968 COVID-19 patients, 81.7% (n=27,741) did not seek medical treatment. Among the 6,227 patients who did receive treatment, 74.0% (n=4,609) chose primary medical institutions, 19.7% (n=1,228) opted for hospitals, and 6.3% (n=390) utilized both primary healthcare facilities and hospitals for their treatment.

The results of the statistical analysis demonstrated that the mean time required to visit primary medical institutions was the lowest at 1.67±0.04 hours, while the mean time to visit hospitals was the highest at 3.75±0.11 hours. The overall mean time to visit both hospitals and primary healthcare facilities was 3.04±0.17 hours.

Univariate analysis demonstrated that the consultation rate of elderly patients (24.2%, 2,134) exceeded that of other age groups, which suggested a preference for treatment among older patients. Additionally, patients with higher education were more inclined (83.9%, 16,867) to select home quarantine following infection. A greater outpatient rate was observed among rural patients (20.4%, 1,845) compared to their urban counterparts, while individuals with co-infections exhibited an outpatient rate of 23.2% (3,777) (Table 1).

A multivariate binary logistic regression analysis was conducted to identify the factors influencing patients' inclination for treatment. Seeking medical treatment was the dependent variable, and gender, age, education level, occupation, residence, and COVID-19-related symptoms were independent variables (Supplementary Table S1, available in http://weekly.chinacdc.cn). After adjusting for other confounding factors, the results of multivariate logistic regression analysis indicated that individuals who were infected with COVID-19 tended to seek medical care at healthcare facilities if they were elderly (*OR*=1.538, 95% *CI:* 1.428–1.657), had a low level of education (*OR*=0.697, 95% *CI:* 0.605–0.805), worked in the service industry (*OR*=0.894, 95% *CI:* 0.803–0.996), or resided in rural areas (*OR*=1.159, 95% *CI:* 1.085–1.237). Fever (*OR*=0.913, 95% *CI:* 0.844–0.989), headache (*OR*=0.893, 95% *CI:* 0.835–0.954), fatigue (*OR*=0.884, 95% *CI:* 0.825-0.948), loss of taste (*OR*=0.929, 95% *CI:* 0.869–0.993), decreased appetite (*OR*=0.995, 95% *CI:* 0.929–1.065), diarrhea (*OR*=0.998, 95% *CI:* 0.922–1.081), and constipation (*OR*=0.919, 95% *CI:* 0.811–1.038) were inversely associated with seeking medical care. Coughing (*OR*=1.379, 95% *CI:* 1.267–1.502), dryness of the pharynx or sore throat (*OR*=1.218, 95% *CI:* 1.138–1.304), runny or stuffy nose (*OR*=1.012, 95% *CI:* 0.950–1.079), muscle pain (*OR*=1.006, 95% *CI:* 0.939–1.078) and joint pain (*OR*=1.033, 95% *CI:* 0.967–1.104), conjunctivitis (*OR*=1.125, 95% *CI:* 0.973–1.297), chest tightness (*OR*=1.602, 95% *CI:* 1.480–1.734), nausea or vomiting (*OR*=1.073, 95% *CI:* 0.990–1.162), difficulty breathing (*OR*=1.347, 95% *CI:* 1.190–1.522), and tachypnea (*OR*=1.384, 95% *CI:* 1.238–1.546) were positively associated with seeking medical care (Table 2).

Patients experiencing symptoms such as dyspnea, elevated respiratory rate, chest tightness, conjunctivitis, and nausea or vomiting were more likely to seek medical consultation. Moreover, individuals with conditions including stroke, cerebrovascular diseases, bronchitis, emphysema, asthma, pneumonia, hepatitis, chronic kidney disease, and cardiac diseases demonstrated a high consultation rate (Supplementary Table S2, available in http://weekly.chinacdc.cn).

Individuals with pre-existing comorbidities displayed the following number of symptoms after infection: hepatitis (7.9±3.7), gastritis/gastric ulcer (7.9±3.3), immunodeficiency diseases (7.8±3.8), bronchitis/emphysema/asthma/pneumonia (7.7±3.5), and tuberculosis (7.7±3.4) (Supplementary Table S3, available in http://weekly.chinacdc.cn). The Kolmogorov-Smirnov (K-S) normality test revealed that the number of symptoms following COVID-19 infection did not adhere to a normal distribution ($P<0.001$), with a median value of 2 symptoms (Figure 1).

For the analysis, the number of pre-existing conditions was categorized using a threshold of 2 symptoms (<2 and ≥2). The results indicated that patients with <2 underlying conditions exhibited 6.2±3.3 post-infection symptoms, whereas patients with ≥2 underlying conditions displayed 6.6±3.3 symptoms. Additionally, the number of symptoms among patients who visited primary care institutions, hospitals, or both was 6.7±3.4, 7.5±3.6, and 7.8±3.7, respectively (Figure 2). The heatmap for visiting institutions suggested that the median number of

TABLE 1. Medical counselling status, and medical care route selection of 33,968 patients with different demographic characteristics infected with COVID-19 — Beijing, China, December 2022.

Variable	Attendances, *n* (%)	Non-attendences, *n* (%)	χ^2	*P*	Hospitals, *n* (%)	Primary care facilities, *n* (%)	Hospitals and primary care facilities, *n* (%)	χ^2	*P*
Gender									
Male	2,018 (18.4)	8,976 (81.6)	0.004	0.95	408 (20.2)	1,475 (73.1)	135 (6.7)	1.59	0.45
Female	4,209 (18.3)	18,765 (81.7)			820 (19.5)	3,134 (74.5)	255 (6.1)		
Age (years)									
18–59	4,093 (16.3)	21,058 (83.7)	273.60	<0.001	794 (19.4)	3,062 (74.8)	237 (5.8)	5.90	0.05
>60	2,134 (24.2)	6,683 (75.8)			434 (20.3)	1,547 (72.5)	153 (7.2)		
Education level									
Elementary school/below	377 (26.7)	1,035 (73.3)			65 (17.2)	285 (75.6)	27 (7.2)		
Junior high school/ high school/junior	2,621 (21.0)	9,839 (79.0)	195.67	<0.001	439 (16.8)	2,036 (77.7)	146 (5.6)	37.66	<0.001
College/technical school Undergraduate/ postgraduate or above	3,229 (16.1)	16,867 (83.9)			724 (22.4)	2,288 (70.9)	217 (6.7)		
Employment status									
Service trade staff	503 (18.4)	2,231 (81.6)			109 (21.7)	369 (73.4)	25 (5.0)		
Medical industry staff	1,720 (17.8)	7,962 (82.2)	2.96	0.23	314 (18.3)	1,314 (76.4)	92 (5.4)	10.57	0.03
Others	4,004 (18.6)	17,548 (81.4)			805 (20.1)	2,926 (73.1)	273 (6.8)		
Area type									
Urban	4,382 (17.6)	20,521 (82.4)	33.55	<0.001	983 (22.4)	3,087 (70.5)	312 (7.1)	97.96	<0.001
Rural	1,845 (20.4)	7,220 (79.7)			245 (13.3)	1,522 (82.5)	78 (4.2)		
History of physical illness									
Chronic disease	2,450 (13.8)	15,254 (86.2)	498.00	<0.001	730 (19.3)	2,784 (73.7)	263 (7.0)	8.39	0.02
Healthy	3,777 (23.2)	12,487 (76.8)			498 (20.3)	1,825 (74.5)	127 (5.2)		

symptoms was 8, 9, and 10 for primary medical institutions, hospitals, and both, respectively (Figure 3).

DISCUSSION

In December 2022, China updated its epidemic prevention and control policy in response to the rising number of COVID-19 infections and medical visits. Government departments collaborated to allocate medical resources and establish a hierarchical diagnosis and treatment strategy. Considering this context, a cross-sectional questionnaire survey was conducted among 354 community health centers in 16 districts of Beijing between December 26 and December 31, 2022. The findings revealed that more than 80% of patients did not seek medical attention, while over 70% of patients opted for primary healthcare facilities for treatment. Higher consultation rates were observed among elderly individuals, those with lower education levels, residents of rural areas, and individuals with comorbidities. Additionally, patients with varying pre-existing comorbidities or COVID-19 symptoms demonstrated different consultation rates and preferences.

The implementation of graded diagnosis and treatment strategies, in conjunction with pre-issued guidelines from government departments (*4*), provides rehabilitation guidance for individuals with COVID-19 in home isolation and directs those with mild cases to primary medical institutions. This approach aids in maintaining a stable and orderly system for diagnosis and treatment, while minimizing the waste of medical resources. The effectiveness of this policy was confirmed in the study, with over 80% of patients opting for self-medication and home-based treatment. This preference can be attributed to the mild clinical manifestations of COVID-19 (*1*) and patient conditions favorable for home-based recovery.

Elderly individuals with COVID-19, due to their underlying health conditions and weakened immune systems, are more likely to seek medical consultation

TABLE 2. Binomial logistic regression analysis of medical counseling status influenced by demographics and symptoms among coronavirus disease 2019 (COVID-19) patients — Beijing, China, December 2022.

Variable	*cOR*	*P*	95% *CI*	*aOR*	*P*	95% *CI*	*AOR*	*P*	95% *CI*
Gender: (ref. Male)									
Female	0.998	0.938	0.941−1.058	1.028	0.373	0.968−1.091	0.973	0.389	0.915−1.035
Age: (ref. 18–59 years)									
≥60 years	1.643	<0.001	1.549−1.743	1.584	<0.001	1.473−1.704	1.538	<0.001	1.428−1.657
Education level: (ref. primary or below)									
Junior high school/high school/junior college/technical school	0.731	<0.001	0.646−0.830	0.857	0.019	0.754−0.976	0.897	0.103	0.788−1.023
Undergraduate/postgraduate or above	0.526	<0.001	0.465−0.595	0.693	<0.001	0.603−0.798	0.697	<0.001	0.605−0.805
Employment status: (ref. service trade staff)									
Medical industry staff	0.958	0.446	0.859−1.070	1.124	0.050	1.001−1.264	1.065	0.300	0.946−1.199
Others	1.012	0.819	0.914−1.122	0.880	0.019	0.792−0.980	0.894	0.040	0.803−0.996
Residence area: (ref. urban)									
Rural	1.197	<0.001	1.126−1.272	1.128	<0.001	1.057−1.203	1.159	<0.001	1.085−1.237
Fever: (ref. no)									
Yes	0.904	0.007	0.839−0.973	0.842	<0.001	0.779−0.910	0.913	0.025	0.844−0.989
Cough: (ref. no)									
Yes	1.477	<0.001	1.365−1.598	1.400	<0.001	1.287−1.525	1.379	<0.001	1.267−1.502
Dry throat/sore throat: (ref. no)									
Yes	1.305	<0.001	1.227−1.388	1.214	<0.001	1.135−1.300	1.218	<0.001	1.138−1.304
Stuffy/runny nose: (ref. no)									
Yes	1.097	0.001	1.038−1.160	0.967	0.293	0.908−1.030	1.012	0.706	0.950−1.079
Painful muscles: (ref. no)									
Yes	1.048	0.117	0.988−1.111	0.991	0.801	0.925−1.062	1.006	0.867	0.939−1.078
Arthralgia: (ref. no)									
Yes	1.114	<0.001	1.054−1.178	1.048	0.163	0.981−1.119	1.033	0.332	0.967−1.104
Headaches: (ref. no)									
Yes	0.968	0.244	0.916−1.023	0.841	<0.001	0.788−0.898	0.893	<0.001	0.835−0.954
Conjunctivitis: (ref. no)									
Yes	1.400	<0.001	1.223−1.602	1.105	0.168	0.957−1.273	1.125	0.107	0.973−1.297
Physical weakness: (ref. no)									
Yes	0.998	0.954	0.943−1.057	0.870	<0.001	0.812−0.933	0.884	<0.001	0.825−0.948
Chest tightness: (ref. no)									
Yes	1.734	<0.001	1.624−1.851	1.599	<0.001	1.478−1.730	1.602	<0.001	1.480−1.734
Decreased or absent sense of taste and smell: (ref. no)									
Yes	1.008	0.780	0.952−1.067	0.891	<0.001	0.834−0.951	0.929	0.031	0.869−0.993
Nausea/vomiting: (ref. no)									
Yes	1.209	<0.001	1.129−1.296	1.067	0.110	0.985−1.155	1.073	0.085	0.990−1.162
Poor appetite: (ref. no)									
Yes	1.097	0.001	1.036−1.160	1.014	0.679	0.948−1.085	0.995	0.875	0.929−1.065
Diarrhea: (ref. no)									
Yes	1.094	0.014	1.019−1.175	0.954	0.242	0.881−1.032	0.998	0.968	0.922−1.081
Constipation: (ref. no)									
Yes	1.089	0.151	0.969−1.224	0.904	0.108	0.799−1.021	0.919	0.179	0.811−1.038
Breathing difficulties: (ref. no)									
Yes	1.989	<0.001	1.787–2.214	1.397	<0.001	1.236−1.577	1.347	<0.001	1.190−1.522
Increased respiratory rate: (ref. no)									
Yes	1.798	<0.001	1.632−1.980	1.369	<0.001	1.226−1.528	1.384	<0.001	1.238−1.546

Note: *cOR*, crude odds ratio, which was a single factor logistic regression coefficient; *aOR*, odds ratio, which was a logistic regression coefficient after adjusting for demographic confounding factors and symptom confounding factors, respectively; *AOR* was the odds ratio adjusted for sex, age, residence, occupation, education and confounding factors such as fever, cough or sputum.
Abbreviation: *CI*=confidence interval.

compared to younger patients. The outpatient rate of infected individuals in rural areas was higher than that of COVID-19 patients in urban areas. Given the weak medical infrastructure in rural areas of China, the capacity for primary medical care and health services was severely tested during the epidemic. In response, the government issued an emergency plan aimed at strengthening the graded and stratified treatment and referral of patients with COVID-19 by strictly implementing the first diagnosis responsibility system and emergency treatment system (*5*).

The implementation of stratified treatment has been vital in combating the COVID-19 pandemic. Primary healthcare institutions categorize health risks into three distinct levels, taking into consideration factors such as age, pre-existing comorbidities, and vaccination status. These institutions offer tiered medical services for individuals infected with COVID-19, ranging from community screening to diagnosis and treatment at community health centers (*6*). The findings of this study indicate that over 70% of infected patients sought care at primary medical institutions due to their expedited waiting time and convenient access to medical services. As a result, these institutions serve essential roles as both "*sentinels*" and "*network bottoms*" in controlling the epidemic (*7*).

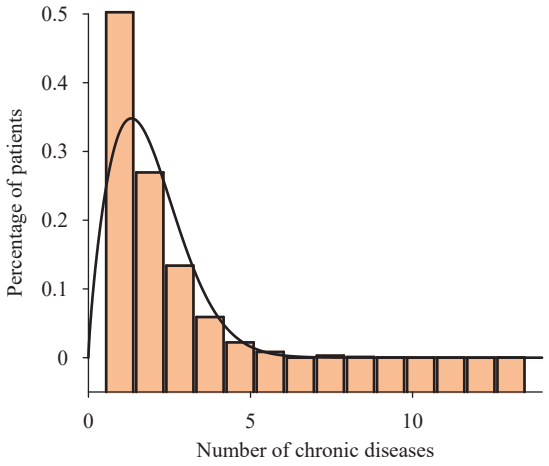

FIGURE 1. The number of chronic diseases in patients with coronavirus disease 2019 (COVID-19) — Beijing, China, December 2022.

This study revealed that patients exhibiting various symptoms opted for different routes when seeking treatment. Those presenting severe symptoms, such as dyspnea, tachypnea, nausea/vomiting, chest tightness, and diarrhea, were more inclined to seek treatment at specialized hospitals. The quantity of symptoms reported post-infection diverged among patients with distinct comorbidities. In accordance with prior research, the mean number of COVID-19 symptoms escalated in correlation to the number of comorbidities. This is consistent with previous studies indicating that pre-existing comorbidities' presence can heighten the risk of complications (*8*) and severe adverse outcomes (*9*). These findings carry significant implications for risk stratification and future strategizing.

Historically, large-scale infectious disease epidemics have led to significant strain on medical resources (*10*). Consequently, effective management of medical resources has emerged as an essential public health concern during such epidemics. The findings of this study suggest that, in the context of large-scale epidemics characterized by high infectivity but low morbidity and mortality, governmental agencies should adopt proactive measures to guide residents in seeking treatment in a graded and stratified manner. This

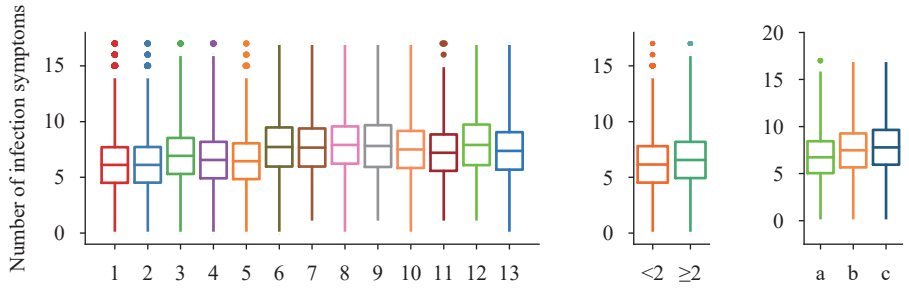

FIGURE 2. Phase diagram illustrating the relationship between the number of coronavirus disease 2019 (COVID-19) symptoms, presence of pre-existing comorbidities, and various medical counseling pathways.
Note: 1=Hypertension; 2=Diabetes; 3=Dyslipidemia; 4=Cardiac disease; 5=Stroke/cerebrovascular disease; 6=Bronchitis/emphysema, asthma/pneumonia; 7=Tuberculosis; 8=Gastritis/gastric ulcer; 9=Immunodeficiency; 10=Arthritis/rheumatism/rheumatoid disease; 11=Chronic kidney disease; 12=Hepatitis; and 13=Cancer. <2 indicates that the number of comorbidities was less than 2; ≥2 indicates that the number of comorbidities was more than 2; a=Primary care facilities; b=Hospitals; c=Hospitals and primary care facilities.

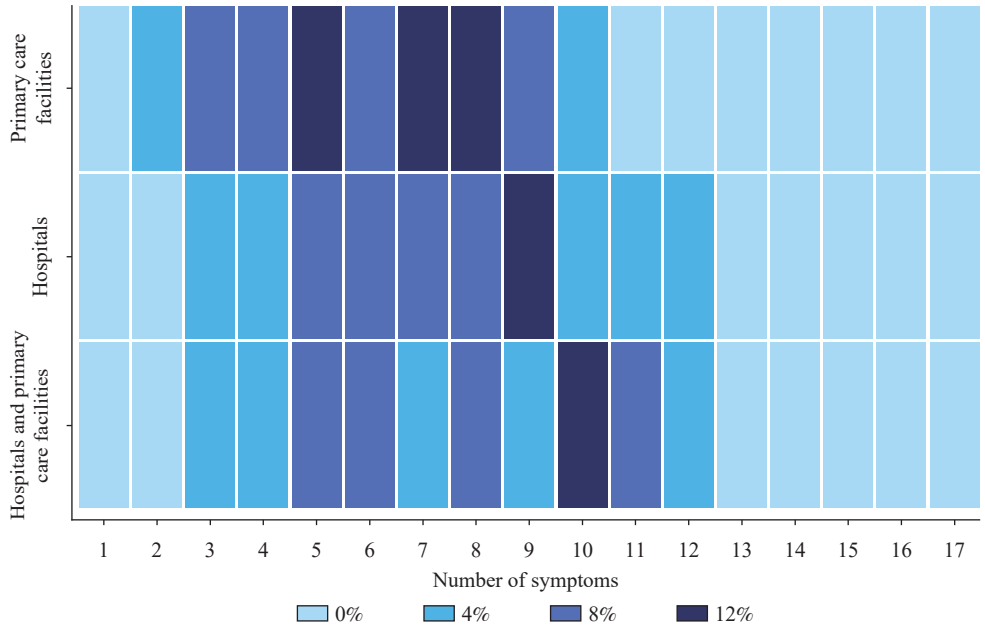

FIGURE 3. Heatmap depicting the prevalence of coronavirus disease 2019 (COVID-19) symptoms according to various medical consultation pathways.

approach would accommodate patient needs while simultaneously reducing the burden on medical resources. Furthermore, enhancing the diagnostic and treatment capabilities of primary healthcare institutions can decrease the influx of patients with minor illnesses at specialized referral hospitals. Consequently, this strategy can alleviate the workload on referral hospitals and establish early warning and referral systems for elderly patients and those with underlying comorbidities.

This study presents several limitations. Despite utilizing a multi-center survey encompassing 33,968 COVID-19 patients from 16 districts in Beijing, potential selection bias must be acknowledged, and extrapolation of the findings should be approached cautiously. Moreover, the study did not specifically examine medications employed by patients during home-based treatment. Consequently, the confounding effects of medication were not accounted for in the multivariate logistic regression model, which could potentially impact the results.

Conflicts of interest: No conflicts of interest.

Funding: Beijing Natural Science Foundation (L222027); Beijing High Level Public Health Technical Talents Training Plan (2022-1-005, Key Discipline Member-02-44).

doi: 10.46234/ccdcw2023.111

[#] Corresponding authors: Hao Wu, wushunzhe@ccmu.edu.cn; Shugang Li, lishugang@ccmu.edu.cn.

[1] School of General Practice and Continuing Education, Capital Medical University, Beijing, China; [2] Department of Epidemiology and Biostatistics, School of Public Health, Peking University, Beijing, China; [3] Beijing Community Health Service Association, Beijing, China; [4] School of Public Health, Capital Medical University, Beijing, China.

Submitted: May 06, 2023; Accepted: June 27, 2023

REFERENCES

1. National Health Commission of the People's Republic of China. Notice on further optimizing the implementation of COVID-19 prevention and control measures. 2022. http://www.gov.cn/xinwen/2022-12/07/content_5730443.htm. [2022-12-7]. (In Chinese).
2. National Health Commission of the People's Republic of China. General strategy for the implementation of "Class B infectious disease under Category B management" of COVID-19 infection. 2023. http://www.nhc.gov.cn/xcs/fkdt/202212/075a30385dff4672b53dd4bf864e3e38.shtml. [2023-1-11]. (In Chinese).
3. National Health Commission of the People's Republic of China. After the implementation of the "Class B infectious disease under Category B management", what are the status of fever clinics, emergency departments, hospitalization and severe treatment in China. 2023. http://www.gov.cn/xinwen/gwylflkjz231/index.htm. [2023-1-14]. (In Chinese).
4. Beijing Municipal Commission of Health. Expert guidance on health management during recovery of persons infected with the novel coronavirus. Beijing: Beijing Chinese Medicine Press. 2023. https://book.kongfz.com/589423/5821907394/. (In Chinese).
5. National Health Commission of the People's Republic of China. Notice on the work plan of implementing a work plan for graded diagnosis and treatment of COVID-19 with medical associations as the carrier. 2022. http://www.gov.cn/xinwen/2022-12/08/content_5730651.htm. [2022-12-8]. (In Chinese).
6. Chinese Society of General Practice, China Association of Traditional Chinese Medicine Branch of General Practice, Respiratory Disease Prevention and Control Speciality Society of Chinese Preventive

Medicine Association, Chinese Alliance for Respiratory Disease in Primary Care, Editorial Board of Chinese Journal of General Practitioners of Chinese Medical Association, Expert Group of Guideline for Diagnosis, Treatment and Management of COVID-19 in Primary Care. Guideline for diagnosis, treatment and management of COVID-19 in primary care (first edition). Chin J Gen Pract 2023;22(2):115 – 37. http://dx.doi.org/10.3760/cma.j.cn114798-20230108-00040. (In Chinese).

7. Zhou R, Yao NL, Chen FF. Roles of primary care in response to the COVID-19 pandemic defined in policy documents. Chin Gen Pract 2022;25(10):1155 – 61,1171. http://dx.doi.org/10.12114/j.issn.1007-9572.2022.0107. (In Chinese).
8. Wang GZ, Yao YP, Shi L, Chen H, Zhang C, Zhen C, et al. Association between major complications and underlying diseases in COVID-19 patients: an analysis of 2079 cases. Acad J Chin PLA Med Sch 2021;42(5):477 – 82. http://dx.doi.org/10.3969/j.issn.2095-5227.2021.05.001. (In Chinese).
9. Zhang YP, Luo W, Li Q, Wang XJ, Chen J, Song QF, et al. Risk factors for death among the first 80543 coronavirus disease 2019 (COVID-19) cases in China: relationships between age, underlying disease, case severity, and region. Clin Infect Dis 2022;74(4):630 – 8. http://dx.doi.org/10.1093/cid/ciab493.
10. Deng W, Dong LY. Collaborative Emergency: “Medical Squeeze”and Cooperative Management in Major Epidemic—Take the COVID-19 Crisis as an Example. Journal of South China University of Technology (Social Science Edition) 2021;23(1):104 – 12. http://dx.doi.org/10.19366/j.cnki.1009-055X.2021.01.011. (In Chinese).

SUPPLEMENTARY MATERIAL

SUPPLEMENTARY TABLE S1. Variable assignment table.

Variable		Variable assignment
Consultations	YI	No=0; Yes=1
Gender	X1	Male=1; Female=2
Age	X2	18–59 years=1; ≥60 years=2
Education level	X3	Primary school or below=1; Junior high school/high school/junior college/technical school=2; Undergraduate/postgraduate or above=3
Employment status	X4	Service trade staff=1; Medical industry staff=2; Others=3
Residence area	X5	Rural=1; Urban=2
Fever	X6	No=0; Yes=1
Cough	X7	No=0; Yes=1
Dry throat/sore throat	X8	No=0; Yes=1
Stuffy/runny nose	X9	No=0; Yes=1
Painful muscles	X10	No=0; Yes=1
Arthralgia	X11	No=0; Yes=1
Headaches	X12	No=0; Yes=1
Conjunctivitis	X13	No=0; Yes=1
Physical weakness	X14	No=0; Yes=1
Chest tightness	X15	No=0; Yes=1
Decreased or absent sense of taste and smell	X16	No=0; Yes=1
Nausea/vomiting	X17	No=0; Yes=1
Poor appetite	X18	No=0; Yes=1
Diarrhoea	X19	No=0; Yes=1
Constipation	X20	No=0; Yes=1
Breathing difficulties	X21	No=0; Yes=1
Increased respiratory rate	X22	No=0; Yes=1

SUPPLEMENTARY TABLE S2. Status of medical counseling and selection of healthcare pathways among COVID-19 patients with varying symptoms and underlying chronic conditions — Beijing, China, December 2022.

Variable	Attendances, *n* (%)	Non-attenders, *n* (%)	Hospitals, *n* (%)	Primary care facilities, *n* (%)	Hospitals and primary care facilities, *n* (%)
Fever	5,179 (18.1)	23,452 (81.9)	1,094 (21.1)	3,751 (72.4)	334 (6.5)
Cough	5,390 (19.3)	22,565 (80.7)	1,070 (19.9)	3,976 (73.8)	344 (6.4)
Dry throat/sore throat	4,584 (19.5)	18,902 (80.5)	862 (18.8)	3,421 (74.5)	310 (6.8)
Stuffy/runny nose	3,668 (18.9)	15,713 (81.1)	729 (19.9)	2,702 (73.7)	237 (6.5)
Painful muscles	4,155 (18.6)	18,221 (81.4)	789 (19.0)	3,097 (74.5)	269 (6.5)
Arthralgia	2,670 (19.3)	11,167 (80.7)	522 (19.6)	1,958 (73.3)	190 (7.1)
Headaches	3,193(18.1)	14,451 (81.9)	654 (20.5)	2,329 (72.9)	210 (6.6)
Conjunctivitis	288 (23.7)	929 (76.3)	58 (20.1)	199 (69.1)	31 (10.8)
Physical weakness	4,003 (18.3)	17,844 (81.7)	856 (21.4)	2,864 (71.6)	283 (7.1)
Chest tightness	1,568 (25.8)	4,509 (74.2)	422 (26.9)	1,006 (64.2)	140 (8.9)
Decreased or absent sense of taste and smell	2,262 (18.4)	10,025 (81.6)	490 (21.7)	1,609 (71.1)	163 (7.2)
Nausea/vomiting	1,273 (20.8)	4,861 (79.3)	343 (26.9)	815 (64.0)	115 (9.0)
Poor appetite	2,398 (19.2)	10,084 (80.8)	573 (23.9)	1,647 (68.7)	178 (7.4)
Diarrhea	1,137 (19.5)	4,703 (80.5)	280 (24.6)	763 (67.1)	94 (8.3)
Constipation	373 (19.6)	1,533 (80.4)	88 (23.6)	253 (67.8)	32 (8.6)
Breathing difficulties	515 (30.0)	1,203 (70.0)	167 (32.4)	299 (58.1)	49 (9.5)
Increased respiratory rate	625 (27.8)	1,621 (72.2)	179 (28.6)	377 (60.3)	69 (11.0)
Hypertension	2,564 (24.1)	8,078 (75.9)	1,924 (75.0)	474 (18.5)	166 (6.5)
Diabetes	1,412 (27.0)	3,824 (73.0)	1,045 (74.0)	263 (18.6)	104 (7.4)
Dyslipidemia	1,279 (23.9)	4,084 (76.2)	927 (72.5)	254 (19.9)	98 (7.7)
Cardiac disease	798 (27.0)	2,155 (73.0)	551 (69.1)	177 (22.2)	70 (8.8)
Stroke/cerebrovascular disease	242 (30.3)	558 (69.8)	160 (66.1)	62 (25.6)	20 (8.3)
Bronchitis/emphysema, asthma/pneumonia	449 (30.0)	1,050 (70.1)	259 (57.7)	142 (31.6)	48 (10.7)
Tuberculosis	21 (24.4)	65 (75.6)	14 (66.7)	4 (19.1)	3 (14.3)
Gastritis, gastric ulcer	432 (24.4)	1,336 (75.6)	289 (66.9)	102 (23.6)	41 (9.5)
Immunodeficiency diseases	27 (26.0)	77 (74.0)	14 (51.9)	5 (18.5)	8 (29.6)
Arthritis/rheumatism/rheumatoid	280 (23.1)	932 (76.9)	206 (73.6)	50 (17.9)	24 (8.6)
Chronic kidney disease	76 (27.5)	200 (72.5)	35 (46.1)	29 (38.2)	12 (15.8)
Hepatitis	30 (29.4)	72 (70.6)	21 (70.0)	8 (26.7)	1 (3.3)
Cancer	94 (20.2)	371 (79.8)	55 (58.5)	28 (29.8)	11 (11.7)

SUPPLEMENTARY TABLE S3. The mean and standard deviation of post-infection symptom number among patients with various chronic diseases and different medical care route selections — Beijing, China, December 2022.

Variable	*n*	COVID-19 symptom number
Chronic disease		
Hepatitis	102	7.9±3.6
Gastritis/gastric ulcer	1,768	7.9±3.3
Immunodeficiency diseases	104	7.8±3.8
Bronchitis/emphysema/asthma/pneumonia	1,499	7.7±3.5
Tuberculosis	86	7.7±3.4
Arthritis/rheumatism/rheumatoid	1,212	7.5±3.3
Cancer	465	7.4±3.4
Chronic kidney disease	276	7.2±3.3
Dyslipidemia	5,363	6.9±3.2
Cardiac disease	2,953	6.6±3.3
Stroke/cerebrovascular disease	800	6.4±3.2
Diabetes	5,236	6.1±3.2
Hypertension	10,642	6.1±3.2
Number of chronic diseases		
<2	8,175	6.2±3.3
≥2	8,089	6.6±3.3
Medical institution		
Hospitals	1,228	7.5±3.6
Primary care facilities	4,609	6.7±3.4
Hospitals and primary care facilities	390	7.8±3.7

Abbreviation: COVID-19=coronavirus disease 2019.

Recollection

Global Overview and Insights on Infodemiology and Infodemic Management

Mingfan Pang[1]; Yichi Zhang[1]; Siyue Guo[1]; Xinping Yang[1]; Xiaopeng Qi[1,#]

The coronavirus disease 2019 (COVID-19) pandemic has underscored the global challenge of managing infodemics. In a situation report published on February 2, 2020, the World Health Organization (WHO) observed that the disease outbreak and response were accompanied by an extensive infodemic, complicating the process for individuals to identify trustworthy sources and obtain reliable guidances during such a critical period (*1*). On February 15, 2020, the Director-General of the WHO, Dr. Tedros Adhanom Ghebreyesus, highlighted the seriousness of this issue by stating, "We're not just fighting an epidemic; we're fighting an infodemic. Fake news spreads faster and more easily than this virus and is just as dangerous (*2*)."

The WHO defines an infodemic as an excessive amount of information during a disease outbreak, which can vary in terms of quality and accuracy. This rapid influx of information may lead to confusion and risk-taking behaviors posing potential health risks. Furthermore, it may cause a decline in trust in health authorities, consequently undermining the effectiveness of public health responses.

Rumors and misinformation have been prevalent throughout human history; however, the COVID-19 pandemic has led to an unprecedented surge of information dissemination compared to previous epidemics. This phenomenon can be partially attributed to the rapid advancements in digital technology and the widespread use of the internet and social media platforms. As of December 2022, the number of internet users in China has reached 1.067 billion, with a coverage rate of 75.6%. Additionally, 99.8% of these users access the internet through cell phones (*3*). In contrast, during the H1N1 influenza pandemic in December 2009, these figures were significantly lower, standing at 0.384 billion, 28.9%, and 60.8%, respectively (*4*).

Individuals depend on both real-world and virtual networks to engage and exchange information, thereby enhancing the effectiveness, range, and influence of information dissemination, regardless of its accuracy. With the increasing diversity of information content, individuals can selectively access information based on their preferences. Concurrently, websites and platforms are inclined to promote content that appeals to users. In the absence of sufficient information and health literacy, individuals may encounter increasingly limited sets of data, inadvertently confining themselves within an information cocoon. This situation makes it challenging to acquire a comprehensive and objective understanding of information.

As understanding and managing infodemics is essential, significant efforts have been made in both research and practice. This article aims to delineate the evolution of infodemiology, present a recommended framework with practical tools for infodemic management, and subsequently discuss the progress and future directions for public health communities in China.

EVOLUTION OF INFODEMIOLOGY

The evolution and significance of infodemiology and infodemics can be understood through four stages of development. Gunther Eysenbach, from the University of Toronto, Canada, first introduced the term "infodemiology" in 2002. At that time, the widespread use of the internet prompted researchers to express concern about the abundance of health information available online, much of which was inaccurate and inconsistent with the best scientific evidence. Consequently, infodemiology emerged as a new research field dedicated to studying the determinants and distribution associated with this phenomenon. The dissemination of health-related information on the internet has resulted in a mixture of both accurate and deceptive sources. In response to this issue, Dr. Eysenbach proposed a conceptual framework that highlights key indicators of information quality, focusing on aspects such as the source, content, and technical features of the information. Moreover, he created the eight-criteria CREDIBLE principle, which serves as a valuable tool for health professionals and

patients to identify and select high-quality online health information (*5*).

In May 2003, David Rothkopf from the United States first introduced the term "infodemic" within a Washington Post article to characterize the "information epidemic" that occurred during the severe acute respiratory syndrome (SARS) outbreak (*6*). Rothkopf emphasized the significant influence of infodemics in transforming SARS from a regional health crisis in China into a global economic and social catastrophe. Through the utilization and amplification of rumors and fear via contemporary information technologies, infodemics has possessed the capacity to affect national and international economies, politics, and security in ways that are vastly disproportionate to the underlying realities.

The third stage emerged around 2006 when infoveillance became a critical approach to disease surveillance and early warning systems. Infoveillance was introduced by Gunther Eysenbach as an expanding area of infodemiology, wherein he developed an information surveillance strategy to monitor flu-related searches on the internet for influenza syndromic surveillance and epidemic prediction. This strategy utilized statistics on ads triggered by keywords "flu" or "flu symptoms" provided by Google Adsense as a proxy for flu-related searches (*7*). In 2009, researchers from Google employed search query data to accurately identify influenza epidemics 1–2 weeks earlier than the CDC's ILI (influenza-like illness) surveillance system, which led to the development of the well-known tool, Google Flu Trends (*8*).

The fourth stage began with the COVID-19 outbreak, during which the WHO acknowledged the infodemic issue and allocated significant resources, engaged multidisciplinary experts, and involved multisector stakeholders in implementing infodemic management, research, and practice. Amidst an information tsunami, factual information, which is accurate and based on current knowledge, contends with misinformation (false information not intended to cause harm) and disinformation (false information created to profit from or cause harm) (*9*). This mixture of misinformation and disinformation, also known as inforus, serves as the driving force behind the infodemic (*10*). The global infodemic management initiative led by the WHO seeks to understand the distribution, determinants, and impact of information, as well as to develop methodologies and tools that foster factual information while counteracting misinformation and disinformation.

FRAMEWORK FOR INFODEMIC MANAGEMENT

Managing an infodemic can be compared to the prevention and control of infectious disease epidemics. In the context of infectious diseases, it is imperative to maintain routine surveillance and emergency preparedness during non-epidemic periods. When an outbreak occurs, the prompt identification of cases and contacts, analysis of transmission modes, implementation of measures to treat cases and prevent new infections, and evaluation of intervention effectiveness are essential. Furthermore, enhancing health systems and increasing the immunity of susceptible populations play a crucial role.

Similarly, managing an infodemic entails several steps. First, consistent monitoring of health knowledge and behavior gaps in the population is crucial, as well as developing infodemic management (IM) capacity within public health institutions. Second, during outbreaks, identifying and tracking rumors, misinformation, and disinformation are essential. The third step involves gathering and translating the best evidence, sharing accurate facts, and debunking false information. Finally, assessing the effectiveness of IM interventions is necessary, in addition to improving the IM system and enhancing the health information literacy of individuals.

The WHO has established distinct competencies for each phase of the epidemic curve (*11*). The infodemic management framework and corresponding competencies are concisely outlined in Table 1.

TOOLS FOR INFODEMIC SURVEILLANCE

Since the beginning of 2020, the WHO has gathered global experts from various disciplines to share knowledge and research findings, develop guidelines, tools, and resources for managing infodemics. These resources are published on their designated infodemic webpages. The initial step in infodemic management involves social listening, which is a labor-intensive task that can be facilitated by information technology. Two prominent digital platforms for public health social listening are the Early AI-supported Response with Social Listening (EARS), developed by the WHO, and the Vaccination Demand Observatory (VDO), created by the United Nations Children's Fund (UNICEF).

TABLE 1. Adapted workstream and competency framework for IM based on WHO Recommendations.

Workstream	Monitor & prepare	Detect	Intervene	Strengthen
Epidemics	Routine disease surveillance and emergency preparedness capacity building.	Promptly detect cases and contacts, and analyze the mode of transmission.	Treat cases and prevent new infections.	Evaluate the impact of interventions; strengthen health systems, and improve population immunity.
Infodemics	Monitor health knowledge and behaviors, and enhance the IM capacity within public health institutions.	Detect misinformation and disinformation, and analyze the spread and impact of infodemics.	Collect and translate the best evidence, share facts, and debunk false information.	Evaluate the impact of IM interventions; strengthen the IM system and improve population health information literacy.
Competencies for infodemic management	1) Social listening to monitor and analyze population knowledge gaps, health behaviors, and determinants; 2) build IM capacity within public health institutions.	1) Fact check to identify mis/disinformation; 2) analyze the impact and factors contributing to infodemics.	1) Identify the most robust evidence, translate scientific findings into high-quality health information, and proactively disseminate information from accurate and reliable sources to target audiences; 2) promptly debunk mis/disinformation; 3) risk communication and community engagement to build trust.	1) Quantify the impact of IM activities; 2) build individual and community resilience against mis/disinformation; 3) strengthen the ability to access high quality health information; 4) enhance the IM system by incorporating data-driven insights and lessons learned, and establish policies, resources, and mechanisms to support its effective implementation.

Abbreviation: IM=infodemic management; WHO=World Health Organization.

In 2021, the WHO introduced its artificial intelligence (AI)-powered social listening tool, EARS. This platform delivers real-time analysis of COVID-19 related narratives from various sources, including Twitter, Facebook, online forums, news articles, and blogs. EARS plays a crucial role in combating the infodemic by proactively identifying emerging topics and information gaps, thus enabling health authorities to address public concerns in a timely manner. The data gathered is automatically classified into 41 categories, such as cause, illness, treatment, and interventions, through a semi-supervised machine learning algorithm. The EARS dashboard enables users to monitor trends over time, categorized by country and WHO region. Presently, EARS performs analyses in nine languages and encompasses 30 countries (*12*).

The UNICEF VDO was established to address the consequences of misinformation and mistrust surrounding vaccines, which have been accentuated by the initiation of COVID-19 vaccination efforts in 2021. In response to the global vaccine hesitancy exacerbated by the infodemic, the VDO supports local communication initiatives by providing insights and evidence-based recommendations for infodemic managers and relevant stakeholders. This tool collects data from both online and offline sources (e.g., surveys, search engine trends, social media, and traditional media) in real-time, utilizing machine learning and natural language processing to identify patterns and monitor trends related to vaccine mis/disinformation. The VDO dashboard allows users to track vaccine misinformation by country of origin, vaccine type, risk level, and specific topics such as side effects and conspiracy theories (*13*).

PROGRESS ON INFODEMIOLOGY AND INFODEMIC MANAGEMENT IN CHINA

Infodemiology has emerged as a significant research topic in China since the COVID-19 pandemic began. Both the National Natural Science Foundation and the National Social Science Foundation have provided funding for research projects related to infodemiology. Although the discipline is still in its early stages, researchers in China have recognized its importance and are contributing to global understanding and best practices. In the Web of Science core collection database, there were a total of 1,481 publications worldwide containing the topic "infodemic" or "infodemiology" from January 1, 2022 to March 31, 2023. An analysis of the publications from the top 10 countries was presented in Table 2. Canadian researchers established the discipline in 2002 with the earliest publications, followed by the United States, which has contributed the largest number of publications to date. Since the year 2020, there has been a sharp increase in the number of publications, with Chinese researchers making significant contributions to the global understanding of infodemic and infodemiology alongside peers from other

TABLE 2. Distribution of the numbers and citation frequency of infodemic/infodemiology publications in the Web of Science Core Collection through March 31, 2023.

Infodemic related publications	USA	China	England	Italy	Spain	Canada	India	Germany	Brazil	Australia
Average times cited per publication	19.07	24.93	15.68	20.98	12.24	48.55	17.14	15.32	4.38	21.77
Total number of publications	388	165	134	128	96	90	90	65	58	56
2023	9	6	4	9	1		2	3	2	3
2022	91	48	32	33	38	27	31	23	19	15
2021	146	63	60	34	24	37	33	25	30	25
2020	92	36	28	26	28	16	23	12	6	12
2019	9	1	2	5	3	3	1	1		
2018	12	2	4	8	1				1	1
2017	5	1	2	3	1					
2016	4	1	2	2		1				
2015	3			5						
2014	5	3		3		1		1		
2013	7	3								
2012	2									
2011	2	1				2				
2009						1				
2004	1					1				
2002						1				

Note: The search query included "infodemic" or "infodemiology" in the title, keywords, or abstract. The number of publications is represented by a color-coded scale, with the highest number in red and the lowest number in green.

countries.

In the context of infodemic management practices, various government levels have worked in conjunction with social media companies to create fact-checking and debunking platforms and tools, referred to as "Piyao" in Chinese. At the national level, the Cyberspace Administration of China (CAC), also known as the Central Cyberspace Affairs Commission, has collaborated with pertinent departments to establish the China Internet Joint Piyao Platform, launched in 2018. Numerous provinces, selected cities, and social media companies, such as Tencent, have also formed their local Piyao platforms. In September 2021, the CAC introduced a proposal aimed at safeguarding cyberspace from disinformation (*14*), and subsequently, in September 2022, executed a three-month special action to combat internet rumors and disinformation in coordination with other relevant organizations and platforms (*15*).

Public health institutions in China are also dedicated to preventing and reducing the risks of infodemics. For instance, China CDC conducts ongoing health education and promotion efforts while also regularly monitoring public opinion since the emergence of COVID-19. In September 2022, the first specialized internal training on infodemic management was held. Currently, there are internal regulations and guidelines under development and nearing completion that address public opinion monitoring and crisis management, major public health information release and risk assessment, and guidance on public opinion related to the internet.

To provide accurate and timely data for public health professionals and decision-makers, China CDC developed an information tool known as the "Global COVID-19 Data Integration and Risk Analysis Platform" in 2021, designed for use by multi-level CDCs in China. This platform aggregates open data from reputable sources worldwide, encompassing information related to COVID-19 cases, deaths, testing, policies, vaccinations, variants, population mobility, and international flights. Advanced technologies facilitate real-time data collection, standardization, visualization, and simulation analysis. In the post-COVID-19 period, the platform will be adapted for use with other diseases that have epidemic potential.

There is a significant need for continued research and development within the realms of infodemiology and infodemic management. The formation of a

specialized team, composed of professionals from various backgrounds, including health, communication, and information technology, is vital for long-term engagement and dedication to both research and practical applications. Moreover, the implementation of a multisector coordination and collaboration mechanism that encompasses public health agencies and non-health organizations is of critical importance for success in this domain.

Ultimately, the primary objective of this research is to enhance media and health information literacy among the general population, thereby fostering a more informed and empowered society.

Conflicts of interest: No conflicts of interest.

Funding: Supported by the National Key R&D Program of China (2021ZD0114101), China-U.S. CDC Cooperation Project (2021NR4), and China Public Health Development Assistance Capacity Building Project.

doi: 10.46234/ccdcw2023.112

[#] Corresponding author: Xiaopeng Qi, qixp@chinacdc.cn.

[1] Center for Global Public Health, Chinese Center for Disease Control and Prevention, Beijing, China.

Submitted: May 05, 2023; Accepted: June 14, 2023

REFERENCES

1. World Health Organization. Novel coronavirus (2019-nCov) situation report-13. 2020. https://www.who.int/docs/default-source/coronaviruse/situation-reports/20200202-sitrep-13-ncov-v3.pdf. [2023-4-21].
2. World Health Organization. Munich security conference. 2020. https://www.who.int/zh/director-general/speeches/detail/munich-security-conference. [2023-4-21].
3. China Internet Network Information Center. The 51st statistical report on the development status of the internet in China. 2023. https://www3.cnnic.cn/n4/2023/0303/c88-10757.html. [2023-4-21]. (In Chinese).
4. China Internet Network Information Center. The 25th statistical report on the development status of the internet in China. 2010. https://www3.cnnic.cn/n4/2022/0401/c88-808.html. [2023-4-21]. (In Chinese).
5. Eysenbach G. Infodemiology: the epidemiology of (mis)information. Am J Med 2002;113(9):763 – 5. http://dx.doi.org/10.1016/S0002-9343(02)01473-0.
6. Rothkopf DJ. When the buzz bites back. 2003. http://www1.udel.edu/globalagenda/2004/student/readings/infodemic.html. [2023-4-22].
7. Eysenbach G. Infodemiology: tracking flu-related searches on the web for syndromic surveillance. AMIA Annu Symp Proc 2006;2006:244-8. https://pubmed.ncbi.nlm.nih.gov/17238340/.
8. Ginsberg J, Mohebbi MH, Patel RS, Brammer L, Smolinski MS, Brilliant L. Detecting influenza epidemics using search engine query data. Nature 2009;457(7232):1012 – 4. http://dx.doi.org/10.1038/nature07634.
9. World Health Organization. Let's flatten the infodemic curve. 2023. https://www.who.int/news-room/spotlight/let-s-flatten-the-infodemic-curve. [2023-4-22].
10. Gao GF. Infodemiology: the science studying infodemic and inforus. China CDC Wkly 2022;4(52):1181 – 2. http://dx.doi.org/10.46234/ccdcw2022.237.
11. World Health Organization. WHO competency framework: building a response workforce to manage infodemics. 2021. https://www.who.int/publications/i/item/9789240035287. [2023-4-23].
12. McGowan BS. World Health Organization's early AI-supported response with social listening platform. J Med Libr Assoc 2022;110(2):273 – 5. http://dx.doi.org/10.5195/jmla.2022.1398.
13. UNICEF. Vaccination Demand Observatory launched to strengthen local communication programmes to address vaccine misinformation. 2021. https://www.unicef.org/press-releases/vaccination-demand-observatory-launched-strengthen-local-communication-programmes. [2023-4-24].
14. The State Council the People's Republic of China. China releases proposal to safeguard cyberspace from disinformation. 2021. https://english.www.gov.cn/statecouncil/ministries/202109/01/content_WS612f625fc6d0df57f98df7d5.html. [2023-4-24]. (In Chinese).
15. Office of the Central Cyberspace Affairs Commission. CAC deployed to carry out the "clear - combat Internet rumors and disinformation" special action. 2022. http://www.cac.gov.cn/2022-09/02/c_1663745754062601.htm. [2023-4-24]. (In Chinese).

Methods and Applications

Detecting SARS-CoV-2 BA.2, BA.4, and BA.5 Variants Utilizing a Robust RT-RPA-CRISPR/Cas12a-Based Method — China, 2023

Meihui Luo[1,&]; Yang Pan[2,&]; Yaqing He[3,&]; Ruhan A[1]; Changcheng Wu[1]; Baoying Huang[1]; Roujian Lu[1]; Li Zhao[1]; Bo Peng[3]; Fei Ye[1]; Huijuan Wang[1]; Yuda Chen[1,4]; Zhen Li[1,5]; Daitao Zhang[2]; Wenling Wang[1,#]; Wenjie Tan[1]

ABSTRACT

Introduction: Since 2019, numerous variants of concern for severe acute respiratory syndrome virus 2 (SARS-CoV-2) have emerged, leading to significant outbreaks. The development of novel, highly accurate, and rapid detection techniques for these new SARS-CoV-2 variants remains a primary focus in the ongoing efforts to control and prevent the coronavirus disease 2019 (COVID-19) pandemic.

Methods: Reverse transcription-recombinase polymerase amplification combined with the clustered regularly interspaced short palindromic repeats-associated protein 12a (CRISPR/Cas12a) system was used to validate the detection of the Omicron BA.2, BA.4, and BA.5 variants of SARS-CoV-2.

Results: Our results demonstrate that the CRISPR/Cas12a assay is capable of effectively detecting the SARS-CoV-2 BA.2, BA.4, and BA.5 variants with a limit of detection of 10, 1, and 10 copies/μL, respectively. Importantly, our assay successfully differentiated the three SARS-CoV-2 Omicron strains from one another. Additionally, we evaluated 46 SARS-CoV-2 positive clinical samples consisting of BA.2 (n=20), BA.4 (n=6), and BA.5 (n=20) variants, and the sensitivity of our assay ranged from 90% to 100%, while the specificity was 100%.

Discussion: This research presents a swift and reliable CRISPR-based method that may be employed to track the emergence of novel SARS-CoV-2 variants.

The Omicron variants of severe acute respiratory syndrome virus (SARS-CoV-2), first identified in Botswana and South Africa in November 2021, rapidly became the predominant global strain, supplanting the Delta variant and presenting several sub-strains, including BA.2, BA.4, and BA.5 (*1*). These sub-strains exhibited numerous mutations and exhibited substantial immune evasion capabilities, increasing the potential for recurrent Omicron infections (*2*). Multiplex real-time reverse transcription-polymerase chain reaction (rRT-PCR) has been employed to detect SARS-CoV-2 variants with *S*-gene mutations (*3*–*4*). However, rRT-PCR assays can be time-consuming and necessitate specialized equipment and high-standard laboratories that many developing countries lack.

As a result, the clustered regularly interspaced short palindromic repeats (CRISPR) and CRISPR-associated protein (CRISPR/Cas) system-based nucleic acid detection method has been adopted for practical application. The CRISPR/Cas12a assay relies on the protospacer adjacent motif (PAM) sites (5'-TTTN-3'), formed by mutations at base 9,866 on the *ORF1ab* gene of the BA.2 variant, base 27,788 on the *ORF7b* gene of the BA.4 variant, and base 26,529 on the *M* gene of the BA.5 variant. Additionally, specific single-base mutations occurred at base 23,040 on the *S* gene of the BA.2 variant and base 27,889 of the BA.5 variant, both of which contained a nearby PAM site. These mutations can be utilized for the precise detection of BA.2, BA.4, and BA.5 variants.

In this study, we designed and analytically validated a method combining reverse transcription-recombinase polymerase amplification (RT-RPA) and CRISPR/Cas12a technology to differentiate SARS-CoV-2 Omicron BA.2, BA.4, and BA.5 variants from one another.

METHODS

Samples

In this study, the specificity of the RT-RPA-CRISPR/Cas12a assay was assessed using wild-type SARS-CoV-2, its variants of concern (VOCs) including Delta and Omicron (BA.1, BA.2, BA.4, and BA.5), as well as influenza strains H7N9, PR8, and X31. Viral nucleic acids were prepared in the laboratory for the assay. Beijing CDC provided twenty samples each of BA.2 and BA.5, while Shenzhen CDC

supplied six BA.4 samples. Additionally, negative clinical samples were obtained from staff at China CDC.

Identifying RT-RPA Primers and CRISPR-RNA (crRNA) Recognition Sequences

Specific mutation sites for the Omicron BA.2, BA.4, and BA.5 variants were identified using the covSPECTRUM webpage and mutation site information provided by the World Health Organization (WHO) (*5*–*7*). The reference genome sequence for SARS-CoV-2 was acquired from the National Centre for Biotechnology Information (NCBI) under the accession number NC_045512.2, and information on mutations in SARS-CoV-2 variants was sourced from Global Initiative on Sharing All Influenza Data (GISAID) (https://www.gisaid.org/). Genomic sequences of BA.2, BA.4, and BA.5 with GISAID accession numbers 12386761, 13651679, and 14253379, respectively, were used as reference sequences for designing RT-RPA primers and crRNA. The BA.2-specific nucleotide mutation sites (C9866T and A23040G), the BA.4-specific nucleotide mutation site (G27788T), and the BA.5-specific nucleotide mutation sites (G26529A and C27889T) were selected for further identification of crRNA recognition sequences containing a PAM sequence with 18 or 20 nucleotides. The resulting RT-RPA amplification products ranged from 100–500 base pairs in length (Figure 1).

RT-RPA Amplification

Reverse transcription isothermal amplification was performed using a commercial RT-RPA kit (AMP-Future Biotech Co. Ltd., Weifang, China). There was 29.4 μL of Buffer A, 2 μL of forward and reverse primers (10 μmol/L) (Table 1), 5 μL of the sample, 2.5 μL of Buffer B, and 9.1 μL of nuclease-free in a 50 μL reaction mixture. Thermal cycling was performed at 42 °C for 30 min.

Preparation of crRNA

The crRNA sequences were designed for the CRISPR/Cas12a assay (Table 1) (*8*). crRNAs were transcribed by annealing DNA oligonucleotides (T7-gRNA-oligonucleotide), which contained a T7 promoter, conserved stem-loop sequences, and guide sequences with a specific DNA oligonucleotide. The synthesis of crRNAs was conducted at 37 °C for 4 hours using a RiboMAX™ Large Scale RNA

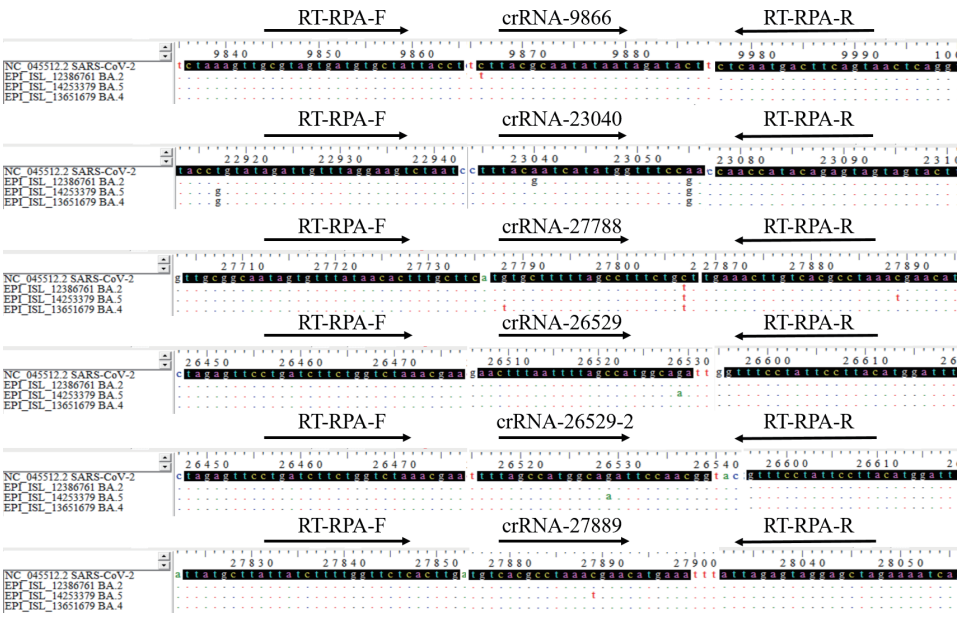

FIGURE 1. Sequence alignment of the SARS-CoV-2 reverse transcription-recombinase polymerase-amplified target region genes with BA.2, BA.4, and BA.5 variants.
Note: The reference sequence used is NC_045512.2 SARS-CoV-2 strain. This figure displays the nucleotide positions of the reference genome amplification target region within the whole-genome sequence. Dots represent nucleotides identical to the reference genome sequence, with mismatched sequences denoted by "a", "t", "c," or "g". Arrows indicate the direction and sequence of upstream primers, downstream primers, and CRISPR-RNA (crRNA) recognition sites.

TABLE 1. List of the reverse transcription-recombinase polymerase amplification (RT-RPA) primers and CRISPR-RNA (crRNA) sequences.

Gene/nucleotide mutation site	Primers/crRNA and template sequence	Sequence (5'–3')
C9866T	RT-RPA-F	CTAAAGTTGCGTAGTGATGTGCTATTACCT
	RT-RPA-R	TCAGAACCTGAGTTACTGAAGTCATTGAGA
	crRNA-9866	UAAUACGACUCACUAUAGGGUAAUUUCUACUAAGUGUAGAUCGCAAUAUAAUAGAUACU
	crRNA-9866 template	AGTATCTATTATATTGCGATCTACACTTAGTAGAAATTACCCTATAGTGAGTCGTATTA
A23040G	RT-RPA-F	TACCTGTATAGATTGTTTAGGAAGTCTAAT
	RT-RPA-R	AAAAGAAAGTACTACTACTCTGTATGGTTG
	crRNA-23040	UAAUACGACUCACUAUAGGGUAAUUUCUACUAAGUGUAGAUCGAACAUAUGGUUUCCGA
	crRNA-23040 template	TCGGAAACCATATGTTCGATCTACACTTAGTAGAAATTACCCTATAGTGAGTCGTATTA
	crRNA-23040-1	UAAUACGACUCACUAUAGGGUAAUUUCUACUAAGUGUAGAUCGAUCAUAUGGUUUCCGA
	crRNA-23040-1 template	TCGGAAACCATATGATCGATCTACACTTAGTAGAAATTACCCTATAGTGAGTCGTATTA
	crRNA-23040-2	UAAUACGACUCACUAUAGGGUAAUUUCUACUAAGUGUAGAUCGAACAUAUGGUUUCCGACC
	crRNA-23040-2 template	GGTCGGAAACCATATGTTCGATCTACACTTAGTAGAAATTACCCTATAGTGAGTCGTATTA
	crRNA-23040-3	UAAUACGACUCACUAUAGGGUAAUUUCUACUAAGUGUAGAUCGAUCAUAUGGUUUCCGACC
	crRNA-23040-3 template	GGTCGGAAACCATATGATCGATCTACACTTAGTAGAAATTACCCTATAGTGAGTCGTATTA
G27788T	RT-RPA-F	TTGCGGCAATAGTGTTTATAACACTTTGCTTC
	RT-RPA-R	ATTTCATGTTCGTTTAGGCGTGACAAGTTTCA
	crRNA-27788	UAAUACGACUCACUAUAGGGUAAUUUCUACUAAGUGUAGAUCUUUUUAGCCUUUCUGUU
	crRNA-27788 template	AACAGAAAGGCTAAAAAGATCTACACTTAGTAGAAATTACCCTATAGTGAGTCGTATTA
G26529A	RT-RPA-F	TAGAGTTCCTGATCTTCTGGTCTAAACGAA
	RT-RPA-R	GAAGACAAATCCATGTAAGGAATAGGAAAC
	crRNA-26529	UAAUACGACUCACUAUAGGGUAAUUUCUACUAAGUGUAGAUCCAUGGCUAAAAUUAAAGUU
	crRNA-26529 template	AACTTTAATTTTAGCCATGGATCTACACTTAGTAGAAATTACCCTATAGTGAGTCGTATTA
	crRNA-26529-1	UAAUACGACUCACUAUAGGGUAAUUUCUACUAAGUGUAGAUGGCAUGGCAAAUUUCCAAC
	crRNA-26529-1 template	GTTGGAATTTGCCATGCCATCTACACTTAGTAGAAATTACCCTATAGTGAGTCGTATTA
	crRNA-26529-2	UAAUACGACUCACUAUAGGGUAAUUUCUACUAAGUGUAGAUGCCUUGGCAAAUUCCAAC
	crRNA-26529-2 template	GTTGGAATTTGCCAAGGCATCTACACTTAGTAGAAATTACCCTATAGTGAGTCGTATTA
	crRNA-26529-3	UAAUACGACUCACUAUAGGGUAAUUUCUACUAAGUGUAGAUGGCAUGGCAAAUUCCAACGG
	crRNA-26529-3 template	CCGTTGGAATTTGCCATGCCATCTACACTTAGTAGAAATTACCCTATAGTGAGTCGTATTA
C27889T	RT-RPA-F	TTATGCTTATTATCTTTTGGTTCTCACTTG
	RT-RPA-R	AGGTGCTGATTTTCTAGCTCCTACTCTAAT
	crRNA-27889	UAAUACGACUCACUAUAGGGUAAUUUCUACUAAGUGUAGAUAAGUUCAUUUAGGCGUGACA
	crRNA-27889 template	TGTCACGCCTAAATGAACTTATCTACACTTAGTAGAAATTACCCTATAGTGAGTCGTATTA

Production System-T7 Kit (Promega, Madison, WI, USA). The resulting crRNA was then purified utilizing the RNeasy Mini Kit (Qiagen, Hilden, Germany) and assessed for purity and concentration using a NanoDrop 2000 spectrophotometer (Thermo Fisher Scientific, Waltham, MA, USA). Finally, samples were aliquoted and stored at −80 °C.

Cas12a-Mediated Assay

Cas12a-mediated target cleavage assays were conducted in a 22 μL reaction volume, using 50 nmol/L LbCas12a (Tolo Biotech, Shanghai, China) preincubated with 100 nmol/L crRNA in 1×TOLOBIO buffer at 37 °C for 10 minutes to form a crRNA-Cas12a complex. Subsequently, 5 μL of RT-RPA product and 500 nmol/L probe reporter (5'-6-

FAM-TTATT-BHQ-1-3') were added, and the mixture was incubated at 37 °C for 20 minutes. The fluorescence signal was monitored every 30 seconds using a fluorescent detector (Kunpeng, Beijing, China). Additionally, the fluorescence signal was scanned with an Amersham ImageQuant 800 (Cytiva, Marlborough, MA, USA).

Digital PCR

Nucleic acid quantification for SARS-CoV-2 was conducted utilizing a digital PCR instrument (Sniper Medical Technology Ltd., Jiangsu, China), with an assay developed in our laboratory (*9*). Samples were examined at four dilutions (ranging from 1,000 to 1 copies/μL) in order to determine concentration levels based on the N gene.

Statistical Analysis and Interpretation of Results

The RT-RPA-CRISPR/Cas12a assay yielded positive results when fluorescence levels between cycle 1 and cycle 40 were at least 1.5 times greater than those of the negative control; otherwise, the assay was considered negative. Data processing and graphical representation were performed using GraphPad Prism software (GraphPad, Boston, MA, USA).

Results

Specificity Assessment

We developed crRNA-9866 to identify the BA.2 variant (Figure 2A). Since Cas12a detection relies on the presence of a PAM site, the targeted locus 9,866 features a single-nucleotide C/T mutation at position nt9866 in the SARS-CoV-2 ORF1ab gene. This leads to the emergence of the PAM sequence in the BA.2 variant, which subsequently activates the trans-cleavage activity of Cas proteins and cleaves fluorescent reporter molecules. We employed this characteristic to differentiate BA.2 strains; however, this site exhibited cleavage activity for both BA.2 and other SARS-CoV-2 strains, without demonstrating specificity (Figure 2A).

We designed an 18 bp-long crRNA by introducing a transition mismatch in crRNA-23040 at position 4, which yielded negative results (Figure 2B). To enhance efficiency, we designed an unmodified transition mismatch crRNA-23040-1 at position 4, along with a 20 bp-long crRNA line consisting of both a transition mismatch in crRNA-23040-2 and an unmodified transition mismatch in crRNA-23040-3 at the same position. The results demonstrated that crRNA-23040-1 and crRNA-23040-3 detected both BA.2 and other subtypes of SARS-CoV-2 strains, thus displaying no specific cleavage ability (Figure 2C, E). However, BA.2 exhibited significant cleavage in the presence of crRNA-23040-2, while no cleavage was observed among other SARS-CoV-2 subtypes (Figure 2D, L). These findings indicate that crRNA-23040-2 can specifically identify BA.2 variants.

The locus 27,788 is distinguished by a single-nucleotide mutation (G/T) at position nt27788 in the SARS-CoV-2 ORF7b gene, which generates the PAM sequence in the BA.4 lineage. Consequently, the crRNA-27788 was designed to specifically detect the BA.4 lineage from other SARS-CoV-2 strains. Significant cleavage was observed for BA.4 in the presence of crRNA-27788, while no cleavage was detected for other SARS-CoV-2 subtypes (Figure 2F, M). These results suggest that crRNA-27788 can accurately and specifically identify BA.4 variants.

The BA.5 variant exhibits a mutation at nt26529, resulting in a PAM locus (Figure 2G). To design an 18 bp length, carefully mismatched crRNA-26529-1 and 26529-2 were introduced at positions 2 and 4, respectively, while a 20 bp length was introduced at position 2 for mismatched crRNA-26529-3 and crRNA-27889 (Figure 2H–K). Subsequent analyses revealed that crRNA-26529-2 and crRNA-27889 specifically recognized the BA.5 variant; thus, they were chosen for further evaluation (Figure 2I, K). The CRISPR-Cas12a mediated triple-line lateral flow assay, coupled with multiplex RT-RPA reactions, has been suggested as a platform for rapid, simultaneous two-gene detection of SARS-CoV-2 in point-of-care testing, which could significantly enhance detection accuracy and efficiency (*10*). Consequently, to improve detection efficiency, crRNA-26529-2 and crRNA-27889 were combined to form crRNA-26529-2-27889 for dual-gene detection of BA.5 (Figure 2N). This demonstrates that crRNA-26529-2-27889 can specifically identify BA.5 variants.

Sensitivity and Repeatability Evaluation

The crRNA-23040-2, crRNA-27788, and crRNA-26529-2-27889 were chosen for the final evaluation of the assay due to their enhanced sensitivity. The respective limits of detection for these crRNAs were 10, 1, and 10 copies/μL (Figure 3). Fluorescence readings demonstrated consistency across the three replicate experiments, and the limits of detection exhibited strong reproducibility (Figure 3G–I).

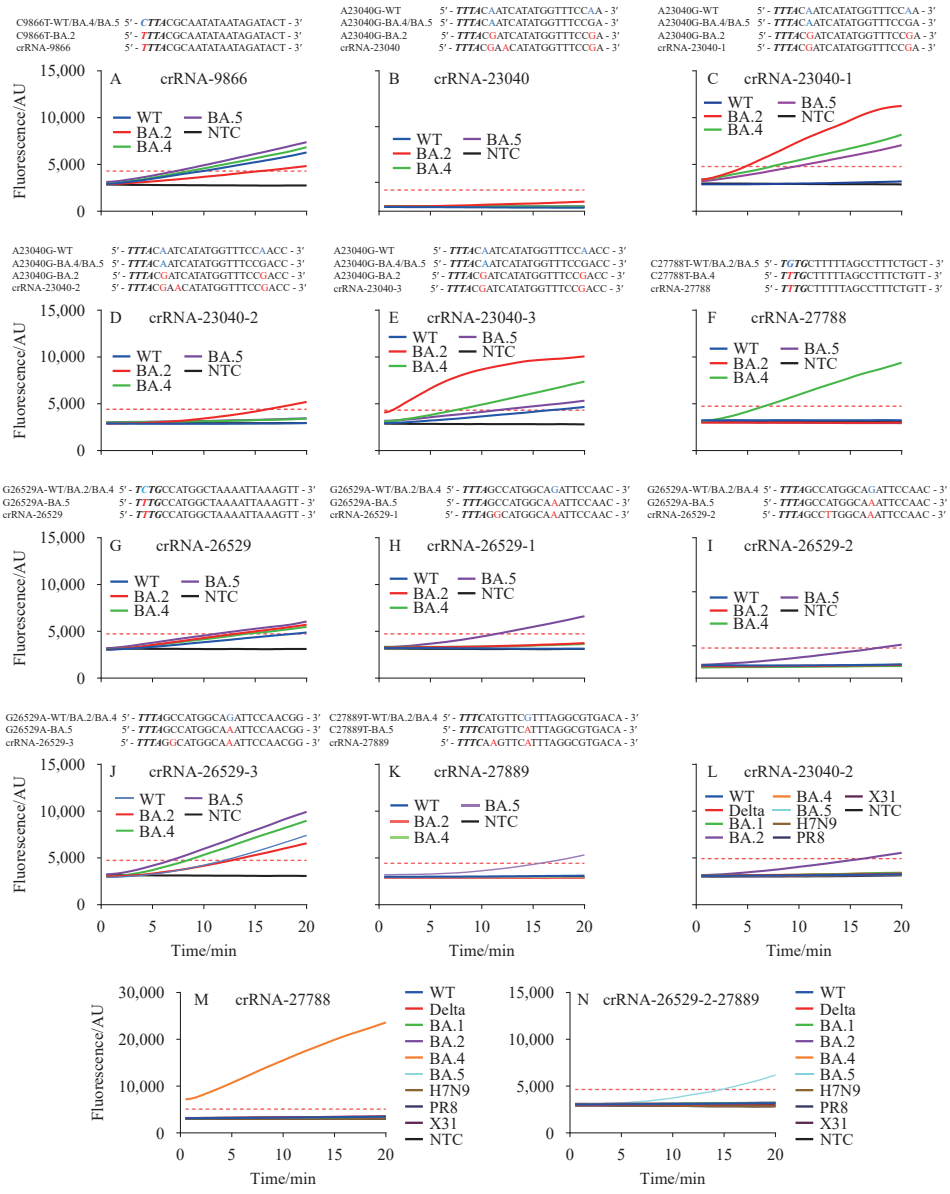

FIGURE 2. Specific identification of SARS-CoV-2 BA.2, BA.4, and BA.5 strains using Cas12a cis-cleavage and trans-cleavage by specific CRISPR-RNA (crRNA). (A) In vitro cleavage assay of C9866T targets using an 18 bp crRNA-9866 to detect BA.2 strains. (B) In vitro cleavage assay of A23040G targets using crRNA-23040 to detect BA.2 strains. An 18 bp crRNA-23040 by introducing a "T to A" transition mismatched at position 4 of the crRNA. (C) In vitro cleavage assay of A23040G targets using an 18 bp crRNA-23040-1 to detect BA.2 strains. (D) In vitro cleavage assay of A23040G targets using crRNA-23040-2 to detect BA.2 strains. A 20 bp crRNA-23040-2 by introducing a "T to A" transition mismatched at position 4 of the crRNA. (E) In vitro cleavage assay of A23040G targets using a 20bp crRNA-23040-1 to detect BA.2 strains. (F) In vitro cleavage assay of C27788T targets using an 18 bp crRNA-27788 to detect BA.4 strains. (G) In vitro cleavage assay of G26529A targets using a 20bp crRNA-26529 to detect BA.5 strains. (H) In vitro cleavage assay of G26529A targets using crRNA-26529-1 to detect BA.5 strains. An 18bp crRNA-26529-1 by introducing a "C to G" transition mismatched at position 2 of the crRNA. (I) In vitro cleavage assay of G26529A targets using crRNA-26529-2 to detect BA.5 strains. An 18 bp crRNA-26529-2 by introducing an "A to T" transition mismatched at position 4 of the crRNA. (J) In vitro cleavage assay of G26529A targets using crRNA-26529-3 to detect BA.5 strains. A 20 bp crRNA-26529-3 by introducing a "C to G" transition mismatched at position 2 of the crRNA. (K) In vitro cleavage assay of C27889T targets using crRNA-27889 to detect BA.5 strains. A 20 bp crRNA-27889 by introducing a "T to A" transition mismatched at position 2 of the crRNA. (L) Verification of the specificity of crRNA-23040-2 for BA.2 with other variants of SARS-CoV-2 and influenza viruses. (M) Verification of the specificity of crRNA-27788 for BA.4 with other variants of SARS-CoV-2 and influenza viruses. (N) Verification of the specificity of crRNA-26529-2-27889 with other variants of SARS-CoV-2 and influenza viruses.
Abbreviation: WT=wild-type nucleic acids; AU=Arbitrary Unit; NTC=negative control.

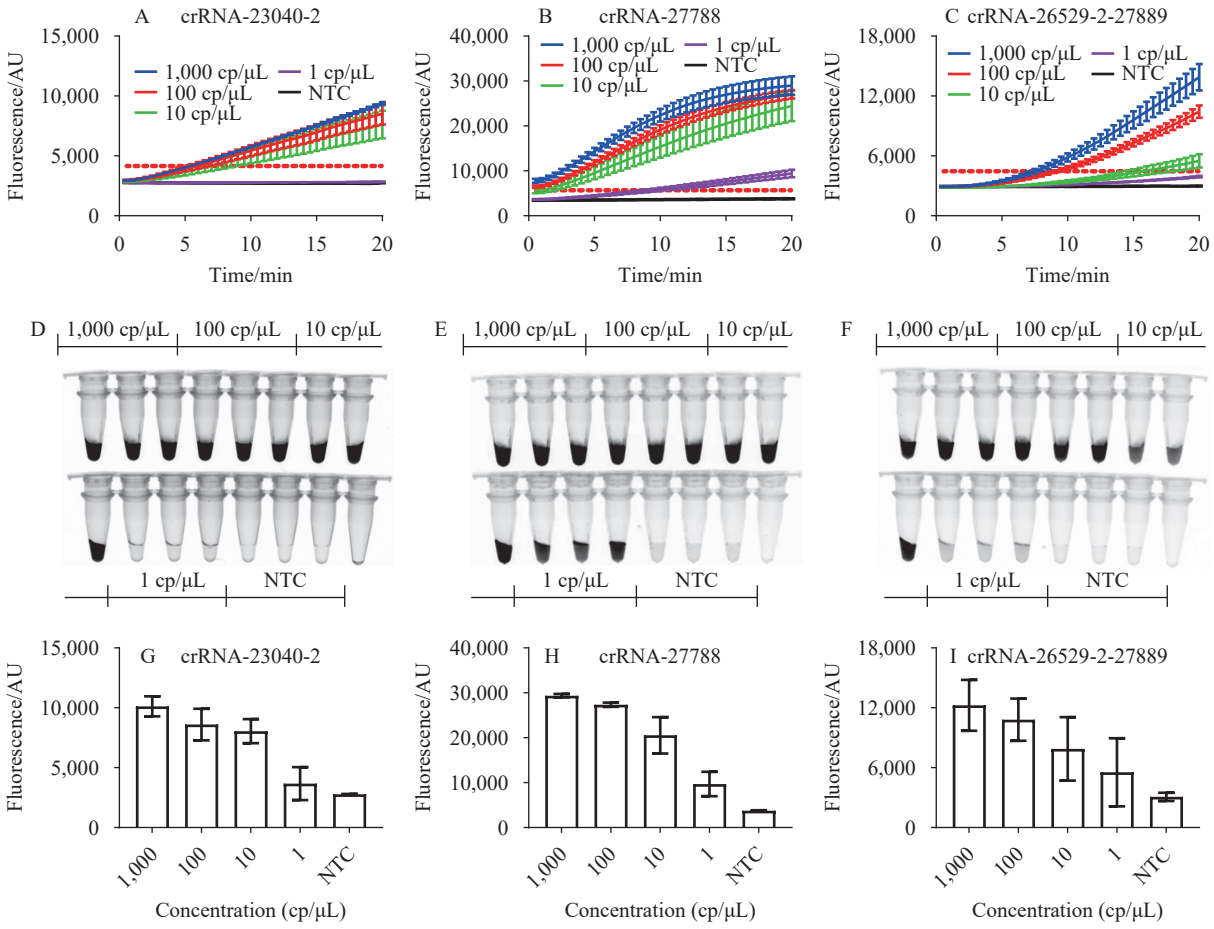

FIGURE 3. Sensitivity and repeatability evaluation. (A–C) LOD for Cas12a fluorometric detection method. (D–F) LOD for Cas12a imager-based detection method. (G–I) Results from three replicate experiments, showing mean fluorescence values obtained in three independent trials.
Abbreviation: AU=Arbitrary Unit; cp=copies; NTC=negative control; LOD=limit of detection.

Evaluation of Cas12a Detection Assay Performance using Clinical Samples

A total of 46 SARS-CoV-2 variant RNA samples, previously analyzed by next-generation sequencing, were examined using the established assay. Each sample was subjected to triplicate RT-RPA reactions in order to detect the presence of BA.2, BA.4, or BA.5 variants. The results demonstrated that the BA.4 and BA.5 assay systems accurately identified all BA.4 (n=6) and BA.5 (n=20) clinical samples with 100% sensitivity and specificity. In contrast, the BA.2 assay missed two out of 20 samples, yielding a sensitivity of 90% and specificity of 100% (Figure 4).

DISCUSSION

The sensitivity of crRNA detection for single-base mutations varies depending on the position and length of the mutations (*11*). Huang et al. demonstrated that the specificity of crRNA binding in the SARS-CoV-2 typing assay was closely correlated with the seed region of the crRNA when single-base mismatches were introduced (*12*). In the current study, we compared two BA.2 crRNAs of differing lengths (18 and 20 bp) with and without single-base mismatches. Results showed that crRNAs of both lengths, without mismatches, cleaved both BA.2 and other mutant strains, while 20 bp crRNAs with single-base mismatches specifically detected BA.2.

CRISPR/Cas detection depends on PAM sites, which can be mutated by the addition of PAM sites. In this study, the locus 27,788 mutation added to the PAM sites, facilitating BA.4 detection. For the BA.5 variant, two loci (26,529 and 27,889) were selected. Locus 27,889 was designed with a single-base mismatch in the 20 bp crRNA, while locus 26,529 was designed to introduce or omit a single-base mismatch at 18 bp and 20 bp, respectively. Both crRNA-26529-

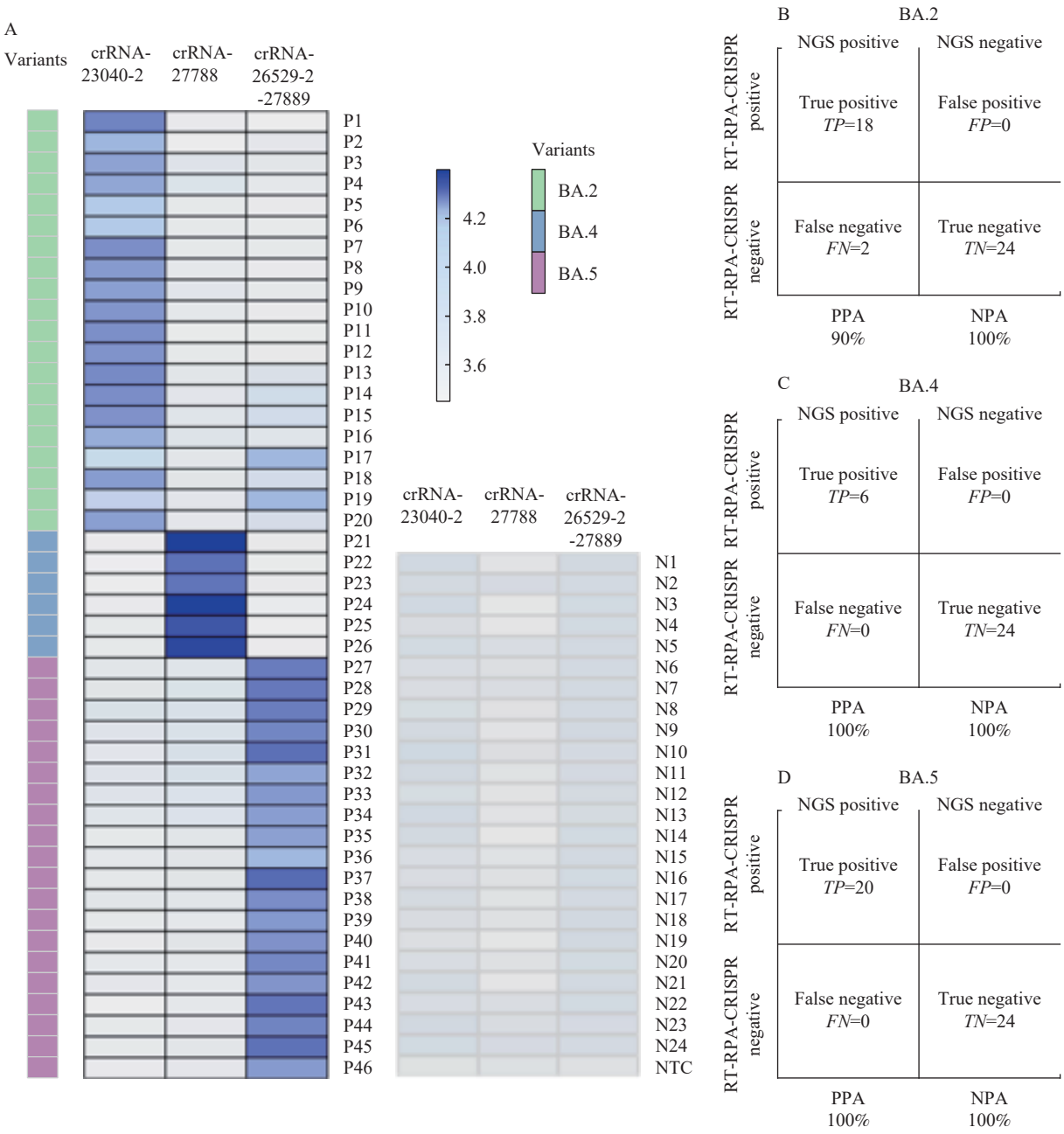

FIGURE 4. Detection of SARS-CoV-2 BA.2, BA.4, and BA.5 in clinical samples using the CRISPR/Cas12a system. (A) Endpoint fluorescence readouts for the reverse transcription-recombinase polymerase amplification (RT-RPA-CRISPR) detection assay were obtained from clinical samples. (Left) Nasopharyngeal swab extracts from 46 positive and (Right) 24 negative patients, as determined by next-generation sequencing, were tested. Blue colors represent a positive result. (B) Sensitivity and specificity of the RT-RPA-CRISPR assay for detecting BA.2. (C) Sensitivity and specificity of the RT-RPA-CRISPR assay for detecting BA.4. (D) Sensitivity and specificity of the RT-RPA-CRISPR assay for detecting BA.5.

2 and crRNA-27889 specifically detected the BA.5 variant.

However, a preliminary assessment demonstrated that the BA.5 detection by crRNAs resulted in weak fluorescence intensity. Consequently, a dual-site detection approach was proposed, combining crRNA-26529-2 and crRNA-27889 as crRNA-26529-2-27889. The crRNA-26529-2-27889 detection of BA.5 variants exhibited high specificity and sensitivity.

The application of Cas12a-based techniques for detecting specific mutations in SARS-CoV-2 has been documented in recent literature. Liang et al.'s CRISPR-based genotyping approach can be employed for identifying the most VOC or variants of interest in

SARS-CoV-2 (*8*,*13*). Fasching et al. targeted L452R, E484K/Q/A, and N501Y mutant loci within the *S* gene to identify the most widespread VOC or variant of interest, including those containing Omicron (*14*). However, only a limited number of methods or algorithms currently exist for genotyping SARS-CoV-2 Omicron subtype strains. The present study has revealed that CRISPR-based genotyping techniques are effective in classifying BA.2, BA.4, and BA.5 subtypes of SARS-CoV-2 Omicron strains.

The CRISPR system employed in this study effectively discriminated between mutations present in the SARS-CoV-2 BA.2, BA.4, and BA.5 variants, exhibiting high sensitivity. Additionally, a consistent level of sensitivity was observed through both fluorescence signal readout and imaging for the BA.2, BA.4, and BA.5 variants, surpassing that of the NASBA-based combined CRISPR-Cas13a locus detection system (N501Y; 82 copies/response) and the LAMP-CRISPR12 combined detection systems (L452R, E484K/Q/A, and N501Y; 10,000 copies/response) (*14–15*). Sequence analysis revealed that emerging BA.5.2.48, BF.7.14, and BQ.1.1 variants, all subvariants of BA.5, contain the detection sites targeted in our BA.5 analysis, indicating a theoretical potential for detection.

A key limitation of this study, however, was the absence of validation using a substantial set of clinical samples. Additionally, false positives were observed at site 27,889 in some BA.2 samples due to the crRNA seed sequence being specifically identified at alternate locations within the SARS-CoV-2 sequence when single-base mismatches were introduced. Further refinement of the method could enhance assay specificity.

Conflicts of interest: No conflicts of interest.

Funding: Supported by the National Key Research and Development Program of China (2021YFC2300101, 2021YFC0863300, 2022YFC2304101, 2022YFC2303401).

doi: 10.46234/ccdcw2023.113

[#] Corresponding author: Wenling Wang, wangwl@ivdc.chinacdc.cn.

[1] MHC Key Laboratory of Biosafety, National Institute for Viral Disease Control and Prevention, China CDC, Beijing, China; [2] Beijing Center for Disease Prevention and Control, Beijing, China; [3] Microbiology Laboratory, Shenzhen Center for Disease Control and Prevention, Shenzhen City, Guangdong Province, China; [4] School of Public Health, Baotou Medical College, Baotou City, Inner Mongolia Autonomous Region, China; [5] Collaborative Innovation Centre for Regenerative Medicine and Medical BioResourse Development and Application Co-constructed by the Province and Ministry, Guangxi Medical University, Guangxi Zhuang Autonomous Region, China.
[&] Joint first authors.

Submitted: April 08, 2023; Accepted: June 25, 2023

REFERENCES

1. Tuekprakhon A, Nutalai R, Dijokaite-Guraliuc A, Zhou DM, Ginn HM, Selvaraj M, et al. Antibody escape of SARS-CoV-2 Omicron BA.4 and BA.5 from vaccine and BA.1 serum. Cell 2022;185(14):2422 – 33.e13. http://dx.doi.org/10.1016/j.cell.2022.06.005.
2. Cao YL, Yisimayi A, Jian FC, Song WL, Xiao TH, Wang L, et al. BA.2.12.1, BA.4 and BA.5 escape antibodies elicited by Omicron infection. Nature 2022;608(7923):593 – 602. http://dx.doi.org/10.1038/s41586-022-04980-y.
3. Chung HY, Jian MJ, Chang CK, Lin JC, Yeh KM, Chen CW, et al. Emergency SARS-CoV-2 variants of concern: Novel multiplex real-time RT-PCR assay for rapid detection and surveillance. Microbiol Spectr 2022;10(1):e0251321. http://dx.doi.org/10.1128/spectrum.02513-21.
4. Hale R, Crowley P, Dervisevic S, Coupland L, Cliff PR, Ebie S, et al. Development of a multiplex tandem PCR (MT-PCR) assay for the detection of emerging SARS-CoV-2 variants. Viruses 2021;13(10):2028. http://dx.doi.org/10.3390/v13102028.
5. SARS-CoV-2-variants [Internet]. Tracking SARS-CoV-2 variants. 2022. https://www.who.int/docs/default-source/coronaviruse/s.pdf?sfvrsn=990a05c2_14. [2022-12-27].
6. SARS-CoV-2-variants [Internet]. Tracking SARS-CoV-2 variants. 2022. https://www.who.int/docs/default-source/coronaviruse/non_spike_orfs.pdf?sfvrsn=b663c56d_16. [2022-12-27].
7. COV-Spectrum. Comparing BA.2* vs. BA.5 vs. BA.4. 2022. https://cov-spectrum.org/explore/World/AllSamples/from%3D2022-01-01%26to%3D2023-02-08/variants?pangoLineage=BA.2*&pangoLineage1=BA.5&pangoLineage2=BA.4&analysisMode=CompareEquals&. [2022-12-27].
8. Liang YH, Lin HQ, Zou LR, Zhao JH, Li BS, Wang HY, et al. CRISPR-Cas12a-based detection for the major SARS-CoV-2 variants of concern. Microbiol Spectr 2021;9(3):e0101721. http://dx.doi.org/10.1128/SPECTRUM.01017-21.
9. Niu PH, Lu RJ, Zhao L, Wang HJ, Huang BY, Ye F, et al. Three novel real-time RT-PCR assays for detection of COVID-19 virus. China CDC Wkly 2020;2(25):453 – 7. http://dx.doi.org/10.46234/ccdcw2020.116.
10. Xiong EH, Jiang L, Tian T, Hu ML, Yue HH, Huang MQ, et al. Simultaneous dual-gene diagnosis of SARS-CoV-2 based on CRISPR/Cas9-mediated lateral flow assay. Angew Chem Int Ed Engl 2021;60(10):5307 – 15. http://dx.doi.org/10.1002/anie.202014506.
11. Li SY, Cheng QX, Wang JM, Li XY, Zhang ZL, Gao S, et al. CRISPR-Cas12a-assisted nucleic acid detection. Cell Discov 2018;4:20. http://dx.doi.org/10.1038/s41421-018-0028-z.
12. Huang XM, Zhang FM, Zhu K, Lin WJ, Ma WZ. dsmCRISPR: Dual synthetic mismatches CRISPR/Cas12a-based detection of SARS-CoV-2 D614G mutation. Virus Res 2021;304:198530. http://dx.doi.org/10.1016/j.virusres.2021.198530.
13. Liang YH, Lin HQ, Zou LR, Deng XL, Tang SX. Rapid detection and tracking of Omicron variant of SARS-CoV-2 using CRISPR-Cas12a-based assay. Biosens Bioelectron 2022;205:114098. http://dx.doi.org/10.1016/j.bios.2022.114098.
14. Fasching CL, Servellita V, McKay B, Nagesh V, Broughton JP, Sotomayor-Gonzalez A, et al. COVID-19 variant detection with a high-fidelity CRISPR-Cas12 enzyme. J Clin Microbiol 2022;60(7):e0026122. http://dx.doi.org/10.1128/JCM.00261-22.
15. Wang YX, Zhang Y, Chen JB, Wang MJ, Zhang T, Luo WX, et al. Detection of SARS-CoV-2 and its mutated variants via CRISPR-Cas13-based transcription amplification. Anal Chem 2021;93(7):3393 – 402. http://dx.doi.org/10.1021/acs.analchem.0c04303.

Indexed by Science Citation Index Expanded (SCIE), Social Sciences Citation Index (SSCI), PubMed Central (PMC), Scopus, Chinese Scientific and Technical Papers and Citations, and Chinese Science Citation Database (CSCD)

The inauguration of *China CDC Weekly* is in part supported by Project for Enhancing International Impact of China STM Journals Category D (PIIJ2-D-04-(2018)) of China Association for Science and Technology (CAST).

CCDC weekly

Vol. 5 No. 26 Jun. 30, 2023

Responsible Authority
National Health Commission of the People's Republic of China

Sponsor
Chinese Center for Disease Control and Prevention

Editing and Publishing
China CDC Weekly Editorial Office
No.155 Changbai Road, Changping District, Beijing, China
Tel: 86-10-63150501, 63150701
Email: weekly@chinacdc.cn

CSSN
ISSN 2096-7071
CN 10-1629/R1